Analysis of baroreflex functionality in pregnancy through hemodynamical modeling

Master Thesis Nadine Boutkan

October 7, 2024

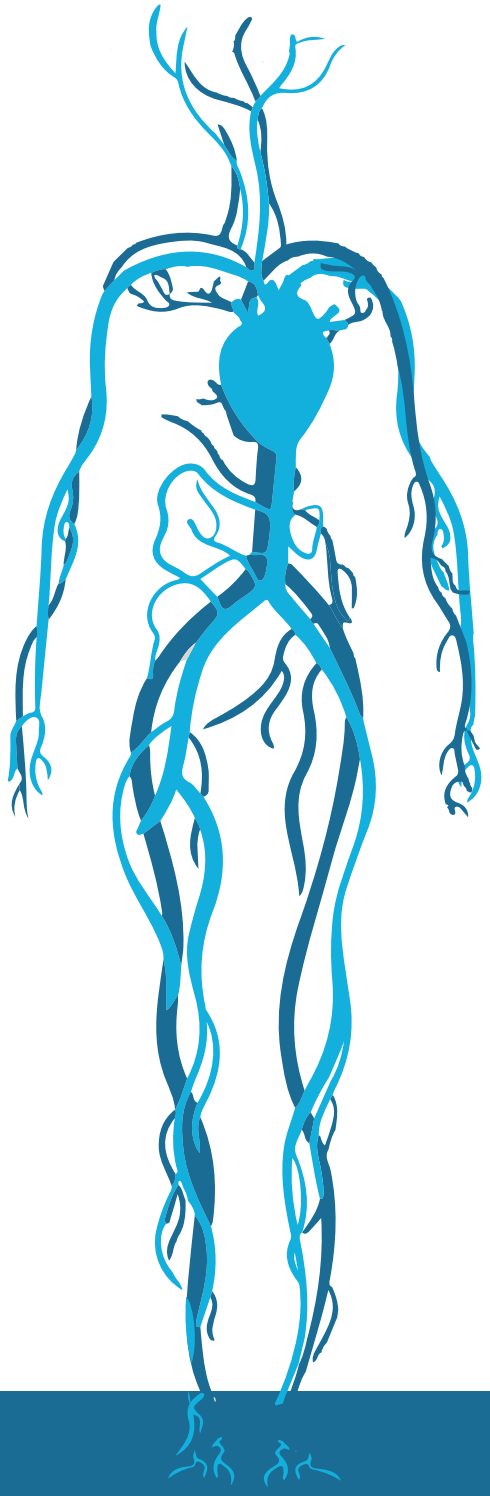

Chair/technical supervisor:	**Prof. dr. H.J. Zwart**
Medical supervisor:	**dr. J. Van Drongelen**
Technical medicine supervisor:	**M. Van Ochten MSc**
Process supervisor:	**drs. N.S. Cramer Bronemann**
External member:	**M.P. Mulder MSc**

Radboudumc university medical center

UNIVERSITY OF TWENTE.

Acknowledgements

I would first like to thank my direct supervisors. Maaike van Ochten who has guided me day to day through all the struggles but also shared the joys I encountered during my internship, as well as Joris van Drongelen, who taught me a lot about the ins and outs of being a medical professional and the additional insights into doing research. Furthermore, also a special thanks to Marc Spaanderman and Ralph Scholten, two gynecologists of the Radboudumc who have helped me especially during the preparations for the presentation of the congress in Florence but were also always available for additional questions and tips.

Of course, I would also like to thank Hans Zwart, my technical supervisor for the critical but wise and practical feedback and keeping me on my own feet. And Nicole Cramer Bornemann, my process supervisor who taught me to accept and defy my own challenges, where my intervision mates Vincent and Veerle as well as Maureen who joined me for so many coffees in the Radboudumc, can not be forgotten.

Lastly, I would like to thank my family, in specific my mother who has been my biggest fan and inspired me to do this research with her experience and enthusiasm for obstetrics. My father for his wise words, and my brother who, now and then, could help me with unasked advice. Also, my great friends and housemates, who listened when I needed to ventilate, but also helped me with several aspects such as creating the front page. I could not have done it alone.

List of abbreviations and model parameters

Abbreviations

MAP	Mean arterial pressure
BRS	Baroreceptor sensitivity
CO	Cardiac output
HR	Heart rate
SV	Stroke volume
VR	Vascular resistance
BP	Blood pressure
PE	Preeclampsia
NE	Norepinephrine
Ach	Acetylcholine
HRV	Heart rate variability
HF	High frequency
LF	Low frequency
mSNA	Muscle sympathetic nerve activity
RAAS	Renin angiotensin aldosterone system
ANGII	Angiotensin II
GABA	Gamma aminobutyric acid
BMI	Body mass index
PV/BSA	Plasma volume corrected for body mass
ms	Milliseconds

Model compartments

AA	Ascending aorta
AD	Descending aorta
AR	Renal arteries
GL	Glomerulus
LA	Left atrium
LB	Lower body
LV	Left ventricle
PA	Pulmonary arteries
PL	Placenta

PV	Pulmonary veins
RA	Right atrium
RV	Right ventricle
SA	Spiral arteries
TU	Renal tubule
UA	Uterine arteries
UB	Upper body
UV	Uterine veins
VC	Vena cava
VR	Renal veins

Model parameters

P	Pressure (mmHg)
V	Volume (L)
E	Elastance ($mmHg*L^{-1}$)
V0	Unstressed volume (L)
Q	Flow ($L*s^{-1}$)
R	Resistance ($mmHg*s*L^{-1}$)
$\bar{p}$	History weighed pressure (mmHg)
N	Baroreceptor firing rate (Hz)
N	Baseline firing rate (Hz)
K	Gain
M	Maximum firing rate (Hz)
τ	Time constant
T_{par},T_{sym}	Parasympathetic and sympathetic tone
β	Dampening factor
C_{ach}, C_{nor}	Acetylcholine and noradrenaline release
H0	Intrinsic heart rate (bpm)
M_s,M_p	Sympathetic and parasympathetic scaling factors
α	Activation factor
Sa	Saturation
Op	Operating point
Th	threshold

Table of Contents

Chapter 1: Introduction

Pregnancy induces crucial cardiovascular adaptations to the maternal system to accommodate increased metabolic demands for both the mother and fetus. Important adaptations include a decrease in peripheral vascular resistance (VR) and blood pressure (BP) and an increase in plasma volume, cardiac output (CO) and heart rate (HR). Through these changes, optimum circumstances are created for placental blood flow to realize fetal growth. Failure to meet these demands can result in hypertensive disorders including preeclampsia (PE), one of the leading causes of morbidity and mortality of mother and fetus [1, 2]. PE is a disease thought to be driven by dysfunction of the placenta, triggering inflammatory and hypertensive reactions of the mother. However, both in presence and absence of PE, other factors also influence the BP during pregnancy [2]. Currently it is known that the arterial baroreflex, which is responsible for the short-term regulation of BP, is diminished during pregnancy. This reduction is even more pronounced in pregnant women with hypertensive disorders such as PE [3-5]. The underlying mechanism behind a diminished baroreflex in pregnancy remains unclear, particularly since the decrease in baroreflex function is even more prominent in a pathological situation. Therefore, more research is necessary to understand the role of the baroreflex in BP maintenance in pregnancy.

To address this knowledge gap, mathematical modeling offers a valuable approach. By simulating cardiovascular changes, models can help clarify the interactions between various physiological processes, including the baroreflex. The Radboudumc is developing a maternal hemodynamic model for this purpose. They have started with a lumped model containing compartments that represent the physiological structures and connectors of the cardiovascular system. Recent work has implemented the renal autoregulation, since this has an important role in maintaining BP and extracellular fluid volume [6]. The model is under constant development where one of the next steps is to implement the baroreflex. Many studies have been performed in modeling the baroreflex within a closed-loop system. For example, Sharifi et al. examined calcium transport within the baroreflex [7], Fernandes et al. studied the afferent pathway's role in action potential propagation [8], and Jezek et al. incorporated lung dynamics as well as the baroreflex into a lumped compartment model [9]. Given the complexity of the cardiovascular system, particularly the baroreflex, each model varies in scope, emphasizing different aspects of the physiology. In this research, we aim to build on these efforts by incorporating mechanisms of the baroreflex that could be altered during pregnancy. Our goal is to enhance the understanding of baroreflex function in pregnancy through the development of a mathematical model that captures its role in BP regulation.

1.1 Outline

This thesis is structured into four chapters. In Chapter 1 we outline the research objective. In Chapter 2 we provide the essential background information, covering the physiology of the BP mechanisms, cardiovascular changes during pregnancy and the baroreflex. In Chapter 3, we present potential influences on reduced baroreflex function. In Chapter 4, the last chapter, we detail the modeling work. We elaborate on our choices in functions for the open-loop model and discuss them further within the closed-loop model.

Chapter 2: Background information

2.1 Blood pressure regulation outside of pregnancy

BP regulation is governed by three primary mechanisms: blood volume, VR, and CO. Blood volume is predominantly controlled by the kidneys, which manage fluid balance through processes such as filtration and reabsorption. In contrast, VR and CO are largely modulated by the baroreflex, a key mechanism for short-term BP regulation. The baroreflex detects changes in BP through specialized receptors (baroreceptors) located in the arterial walls. The baroreflex responds by adjusting both VR and CO through the release of neurotransmitters by the sympathetic and parasympathetic nervous system.

2.1.1 Cardiac output

CO refers to the volume of blood ejected by the heart per minute and is calculated by multiplying stroke volume (SV) with HR. The HR is managed mainly by the baroreflex, while SV depends on more factors, including preload, contractility and afterload.

Preload refers to degree of stretch in the ventricular muscle fibers at the end of diastole, which is mainly dependent on the volume in the ventricles. The amount of volume available for contraction is called venous return. An increase in venous pressure or blood volume in the vena cava enhances venous return, allowing the ventricles to fill more effectively. Factors such as venoconstriction (caused by the baroreflex) and elevated blood volume can increase venous return.

Conversely, increased arterial resistance (afterload) can negatively impact venous return by reducing SV. Afterload refers to the resistance the heart must overcome to eject blood into the aorta and pulmonary arteries. When afterload is elevated, the ventricles struggle to eject sufficient blood, leading to a decrease in SV and ultimately reducing CO. This drop in CO, in turn, lowers venous return, since the two must remain balanced.

The SV is also influenced by contractility, which describes the strength of the heart's contraction. Increased contractility results in a more forceful ejection of blood, thereby increasing SV. Conversely, decreased contractility leaves more blood in the ventricles after contraction, reducing SV and making the heart less efficient.

Eventually CO is the product of SV and HR (the number of beats per minute). When HR increases, CO generally rises because the heart pumps more frequently. However, at higher hear rates, the duration of the filling phase is shortened, reducing venous return regardless of preload and thereby limiting SV and CO.

2.1.2 Heart rate

The HR is regulated by the baroreflex, where neurotransmitters impact pacemaker tissue within the heart. This pacemaker tissue, located in the sinoatrial (SA) node, can spontaneously depolarize and generate an action potential which can trigger contraction. The SA node has an intrinsic firing rate of approximately 60 beats per minute (bpm). So, without the influence of the autonomic nervous system (the baroreflex), the heart initiates an intrinsic HR of 60 bpm.

A heartbeat occurs when the membranes of heart tissue depolarize. The maximum membrane potential is reached during diastole and is around -60 mV. Pacemaker tissues have the ability to gradually depolarize by altering ion flow across the membranes, raising the membrane potential toward a threshold of approximately -40 mV. Once this threshold is reached, more ion channels open, triggering rapid depolarization and the generation of an action potential.

The frequency of this depolarization can be modulated by the autonomic nervous system through the baroreflex. The baroreflex regulates the release of neurotransmitters by the parasympathetic and sympathetic nervous systems. The parasympathetic nervous system facilitates relaxation and energy conservation by slowing the HR and enhancing digestive processes. The parasympathetic nervous system decreases HR by releasing acetylcholine (Ach). The release of Ach can decrease the HR in three different ways. First, it decreases the rate of depolarization, causing the threshold for an action potential to be reached more slowly. Second, the threshold potential is elevated, which requires a higher level of depolarization to trigger an action potential and prolongs the depolarization process. And third, the maximum diastolic potential is lowered, thereby increasing the time required for depolarization. Conversely, the sympathetic nervous system activates the body's stress response, increasing HR, dilating airways, and mobilizing energy for immediate action. The sympathetic nervous system can increase HR by releasing catecholamines (dopamine, norepinephrine, and epinephrine). Catecholamines can solely increase the rate of depolarization, thereby increasing HR, and do not have impact on the threshold or maximum diastolic potential.

2.1.3 Vascular resistance

As described, arterial and venous constriction and dilatation have an indirect influence on BP via pre- and afterload, SV and CO. However, the VR directly influences the BP. Through the release of neurotransmitters of the sympathetic nervous system initiated by the baroreflex, the diameter of vessels can dilate or constrict. The dilation of blood vessels increases their internal diameter, thereby facilitating easier blood flow, resulting in a reduction in blood pressure. Conversely, vasoconstriction, which narrows the vessels, impedes blood flow and leads to an increase in blood pressure due to heightened vascular resistance.

2.2 The baroreflex outside of pregnancy

VR and CO are influenced by the baroreflex. The baroreflex consist of multiple neuronal pathways, which are shown in Figure 1. Afferent vagal and glossopharyngeal fibers collect information from the carotid sinus and aortic arch, where stretch receptors measure changes in BP [10, 11]. The firing rate of these fibers depends on the BP; a rise in BP causes a rise in firing rate and vice versa. Several centers in the medulla, the cardiovascular center of the brain located in the brainstem, respond to the different firing rates of these afferent fibers.

The sensory information is first processed in the nucleus tractii solitarus (NTS), from where the baroreflex splits into a sympathetic and parasympathetic pathway. The sympathetic pathway starts with inhibitory signals to the vasomotor area. The vasomotor area stimulates sympathetic nerves. The sympathetic nerves go to the heart, vessels and adrenal medulla, where they release norepinephrine (NE). NE release at the vessels causes vasoconstriction, has a chronotropic and inotropic effect, and NE release of sympathetic fibers cause the adrenal medulla to release systemic NE in the bloodstream to induce further flight or fight response. So when the baroreflex is stimulated during a rise in BP, the vasomotor area is inhibited, and the sympathetic pathway is less stimulated leading to less vasoconstriction and a decrease in HR and cardiac contractility.

The parasympathetic pathway starts from the NTS with excitatory signals to the cardio inhibitory area (the dorsal motor nucleus of the vagus and the nucleus ambiguus). When the baroreflex is stimulated, the cardio inhibitory area stimulates the parasympathetic nerves travelling mainly to the heart. There, the parasympathetic fibers release acetylcholine (Ach) to nerves close to the SA node, which causes bradycardia. Parasympathetic fibers connected to vessels are far less common compared to sympathetic fibers. They mainly go to the salivary and gastrointestinal glands. Since there are not many parasympathetic fibers going to vessels, the parasympathetic function of the baroreflex is mainly to decrease HR, whilst the sympathetic function is to increase both the HR, cardiac contractility and the VR.

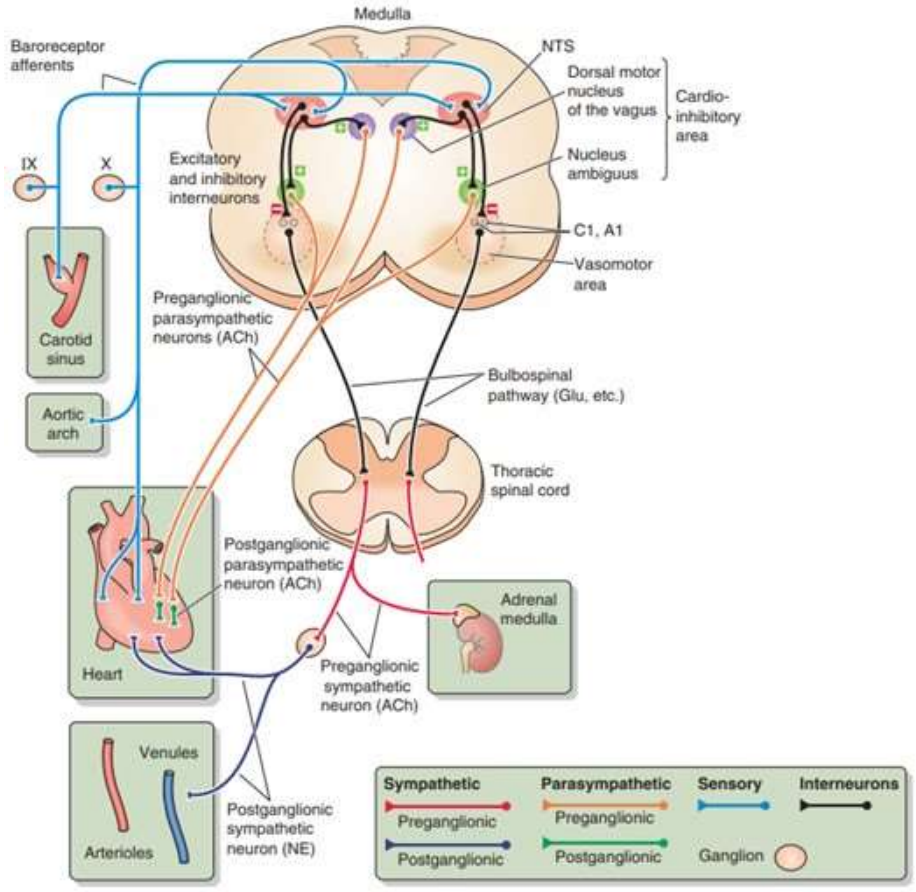

Figure 1: The baroreflex: Afferent fibers from the carotid sinus, aortic arch and the heart stimulate the nucleus tractii solitarus *(NTS) in the medulla. From the NTS, an inhibitory signal goes to the vasomotor area from where sympathetic fibers are stimulated. These fibers release NE at the heart, vessels and adrenal medulla for chronotropic, isotropic and vasoconstrictive effect. An excitatory signal from the NTS goes to the cardio inhibitory area from where parasympathetic fibers are stimulated. These fibers release Ach at the heart causing bradycardia [9].*

2.2.1 The Bowditch effect

The baroreflex also has an indirect influence on cardiac contractility. The cardiac contractility enhances when HR increases, independent of the sympathetic drive stemming from the baroreflex. This distinct physiological phenomenon, known as the "staircase phenomenon" or the "Bowditch effect," was first described by Henry Bowditch in 1871. The mechanism underlying this effect involves an accumulation of intracellular calcium within the cardiac myocytes as HR rises. Calcium plays a critical role in the excitation-contraction coupling process by facilitating cross-bridge formation between actin and myosin filaments, a process essential for muscle fiber contraction. An increased availability of calcium enhances the number of cross-bridges that can form, thereby increasing the contractile force of the heart. The rise in intracellular calcium is attributed to the increased frequency of action potentials at higher heart rates, which allows more calcium to enter the cell during depolarization. Additionally, the repeated influx of calcium enhances its storage within the sarcoplasmic reticulum, further augmenting the calcium reserve available for subsequent contractions and thereby amplifying myocardial contractility [11].

2.3 Baroreflex functionality

One of the most common measures to evaluate the functionality of the baroreflex is called baroreceptor sensitivity (BRS). BRS shows how much the HR responds to a change in BP and is defined as the change in interbeat interval of the HR in ms divided by a unit change in BP in mmHg as shown in Equation 2.1. BRS can be measured through continuous measurements of BP and HR.

$$BRS = \frac{\Delta t\_interbeat}{\Delta BP} \tag{2.1}$$

The effect of the baroreflex on the HR can be evaluated with time domain BRS analysis. However, it is important to notice that the BRS does not take into account the vascular response of the baroreflex, as well as the cardiac contractility response. Furthermore, it is difficult to determine whether the observed effect is due to changes in parasympathetic activity, sympathetic activity, or both [10]. In literature, multiple methods exist to identify contributions of either one of them or both, however it is debated whether these methods are reliable.

A commonly utilized approach for assessing sympathetic and parasympathetic activity induced by the baroreflex is the use of frequency analysis of the heart rate variability (HRV). This allows for the identification of different frequency components within the HRV signal. It is hypothesized that parasympathetic activity predominantly generates high-frequency (HF) signals, as demonstrated in experimental interventions such as vagal stimulation, vagotomy, and muscarinic receptor blockade. In contrast, sympathetic activity is generally associated with low-frequency (LF) signals [12]. This frequency distinction is thought to be attributed to the differing signaling mechanisms of the autonomic nervous system: parasympathetic activity induces faster HR fluctuations through rapid transduction via potassium channels, whereas sympathetic signaling, mediated by beta-adrenergic receptors, occurs more slowly.

However, some studies suggest that LF reflects a combination of both sympathetic and parasympathetic influences, leading to the proposal that the LF/HF ratio may be a more reliable indicator of sympathetic activity. Despite its widespread use, frequency analysis remains limited by the absence of standardization, including the poorly defined cut-off frequencies that separate LF and HF bands. Additionally, factors such as arrhythmias, posture, and respiratory rate can significantly affect HRV measurements, further questioning the validity of this method for accurately assessing autonomic function [13].

Another way to asses sympathetic activity is through direct measurement of muscle sympathetic nerve activity (mSNA) at the peroneal nerve [14]. The amount of burst in the peroneal nerve represents the sympathetic activity. In turn, the sympathetic activity generally reflects the occurring vasoconstriction which is predominantly modulated by the baroreflex. Therefore, the measured mSNA provides valuable insight in the function of the baroreflex. Although this sounds promising, the technique for measuring mSNA is invasive and technically challenging leading to inconsistent result. Furthermore, the mSNA is measured regionally which does not necessarily mean that the overall sympathetic tone is represented.

In summary, the baroreflex can be evaluated through time domain analysis using baroreflex sensitivity (BRS), frequency analysis of HRV, and measurement of muscle sympathetic nerve activity (mSNA). However, due to the unreliable results associated with frequency analysis and mSNA, this study will focus exclusively on BRS for baroreflex assessment.

2.4 Blood pressure regulation during pregnancy

During the first trimester of pregnancy, one of the primary changes occurring in the cardiovascular system is a decrease in VR. This reduction is initially induced by the corpus luteum, a temporary endocrine structure formed during ovulation which produces hormones to support pregnancy. Due to the decrease in VR, the BP also decreases. The large drop in BP triggers fluid-retaining factors such as the renin-angiotensin-aldosterone system (RAAS) which results in an increase in plasma volume. CO rises likewise due to the increased HR, preload and decreased afterload. The decrease in systemic resistance is larger than the increase in CO, eventually leading to a lower BP during pregnancy. The dilated vessels, with low BP, increased plasma volume and CO create optimum circumstances for placental blood flow between mother and fetus. These cardiovascular changes are maintained through other additional factors such as placental hormones, steroids and renal regulation [5, 15]. These hemodynamic changes occur slowly and continuously, which can be seen in Figure 2.

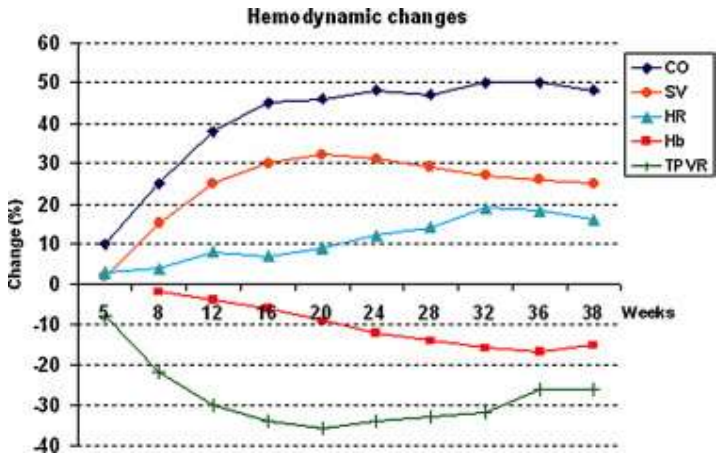

Figure 2: Maternal hemodynamic changes over time course in pregnancy (CO, cardiac output; SV, stroke volume; HR, heart rate; Hb, hemoglobin; TPVR, total peripheral vascular resistance). [11]

2.5 The baroreflex during pregnancy

Increased sympathetic activity and decreased BRS has been shown in pregnant women. These changes are even more pronounced in pregnant women with hypertensive disorders [5]. The underlying reasons for these alterations during pregnancy remain unclear, especially since the methods for studying these alterations lack a golden standard. It is important to note that increased sympathetic activity and decreased BRS may not necessarily result from the same influence; rather, one may be a consequence of the other. Nevertheless, speculations are made for plausible causes of increased sympathetic activity and decreased BRS.

Animal studies have shown that while afferent and efferent activity of the baroreflex remains intact, the brain function of the baroreflex is still altered, which suggest a more central oriented cause. Other influences are also speculated such as the influence of hormones and neurotransmitters.

Hormones, particularly volume-retaining hormones such as the RAAS and vasopressin, are considered strong influential factors on sympathetic activity during pregnancy. Meanwhile, gonadal hormones like progesterone and estrogen show a weak correlation with increased sympathetic activity.

Studies in rats have shown that the pressor and sympathetic responses to AngII in the brain are increased in pregnant rats compared to non-pregnant rats, suggesting a central modification in the brain during pregnancy. This could potentially be caused by an increased expression of AngII receptors found in rats. Moreover, neurotransmitter gamma-aminobutyric acid (GABA) levels and receptors may play an important role. GABA serves as the primary inhibitory factor in the brain region. Alterations in GABA related reactions in the brain have been found in pregnant rats. These changes can cause a decreased inhibition of sympathetic activity [5].

Although these named arguments are primarily derived from animal studies and remain speculative, they point into the direction that central changes combined with altered hormone levels and neurotransmitter function lead to altered sympathetic activity and BRS observed during pregnancy.

Chapter 3: Baroreceptor mediated blood pressure control in women with a history of preeclampsia

Abstract

Objective: Preeclampsia (PE) is associated with increased cardiovascular risk later in life, including diminished baroreceptor sensitivity (BRS), which affects blood pressure (BP) regulation. This study investigated the correlations between cardiovascular variables and BRS, 5 to 10 years postpartum in women with a history of PE compared to healthy controls. Additionally, we explored the mechanisms of BRS during head-up tilt testing.

Methods: Correlations were assessed using linear regression analysis. During the head-up tilt, participants were passively tilted from 0 to 60 degrees on a tilt table, with continuous beat-to-beat monitoring of BP and heart rate (HR).

Results: The study included 66 women with a history of PE and 44 healthy controls. Mean arterial pressure (MAP), HR, vascular resistance (VR), and wall-to-lumen ratio showed correlations with BRS, though with low explained variance. Former PE patients exhibited a larger decrease in MAP, which was associated with lower BRS in this group, a relationship not observed in the control group. A logistic relationship between MAP decrease and BRS was found when both groups were combined.

Conclusions: Reduced BRS is correlated with several cardiovascular variables, but the low explained variance suggests that other factors, such as autonomic nervous system function and sympathetic activity, likely play a significant role. The logistic relationship between MAP decrease and BRS underscores the complexity of the baroreflex.

3.1 Introduction

Currently it is known that the baroreflex functions differently during normotensive and hypertensive pregnancies [3-5]. Additionally, it is known that hypertensive pregnancy is associated with long term cardiovascular consequences, i.e. a diminished baroreceptor sensitivity (BRS) [16]. The mechanisms responsible for the reduced BRS observed after preeclampsia (PE) remain unclear. Understanding these underlying mechanisms holds significant value for our mathematical modeling.

To address this knowledge gap, we examined the influence of various cardiovascular variables on BRS in both healthy controls and formerly PE patients. In addition to identifying factors that influence BRS, we also investigated the impact of altered BRS on the cardiovascular system itself in these two groups. To achieve this, we analyzed data from a head-up tilt test, one of the most commonly used methods to assess hemodynamic responses to orthostatic challenges. By studying both the factors affecting BRS and its consequences on cardiovascular function, we aimed to gain a deeper understanding of the reduced BRS seen in formerly PE patients.

3.2 Methods

We evaluated possible influences of several cardiovascular variables on BRS. The studied variables were: bio mass index (BMI), age, mean arterial pressure (MAP), heart rate (HR), stroke volume (SV), cardiac output (CO), plasma volume corrected for body surface area (PV/BSA), vascular resistance (VR), compliance and wall-to-lumen ratio. The BRS was determined by calculating the mean BRS (eq. 1) of a five-minute rest-period before head-up tilt. We further measured standard cardiovascular variables including the MAP, HR, SV, CO and VR during head-up tilt. The VR was calculated by dividing the MAP by the CO. Additionally we examined age, PV/BSA, and vascular compliance and the wall-to-lumen ratio of the carotid artery. The compliance was calculated by dividing the mean difference in diameter of the carotid artery during systole and diastole by the mean difference in BP during systole and diastole. The wall-to-lumen ratio is defined as the diameter of the wall divided by the diameter of the lumen of the carotid artery. For each of these variables we performed linear regression analysis to study whether the cardiovascular variables might correlate to (reduced) BRS. For the linear regression analysis, we use a Spearman's rho test, which can be used for non-normal distributed data. A $p<0.05$ indicates a correlation coefficient significantly different from zero, and therefore a possible influence. In addition, we plotted the slope and R^2 for better insights on the dependence of BRS on the variable.

To study how altered BRS impacts cardiovascular function, we used data of a head-up tilt test of women with a history of PE 5 to 10 years ago and compared them to women that had a healthy pregnancy. During head-up tilt, the subjects were positioned horizontally on a tilt table and then gradually tilted upward to a 60-degree angle. Beat-to-beat BP and HR measurements were performed during the entire protocol, from which other variables (BRS, CO and VR) could be determined.

We examined the potential influence of BRS on the variation in BP induced by head-up tilt, aiming to uncover possible mechanistic differences between healthy and formerly preeclamptic women. To achieve this, we conducted both linear and logistic regression analyses, to determine which model provides a better fit and thereby assessing the explanatory power of potential relationships. The model fit was evaluated using performance parameters, including the residual sum of squares (RSS), calculated by Equation 3.1, and the R^2, calculated by Equation 3.2. The RSS represents the total of the squared differences between the observed data points and the predicted values in a regression model and indicating the unexplained variance in the data. R^2 reflects the proportion of the variance in the dependent variable that is explained by the independent variables in a regression model. A lower RSS indicates fewer errors between the model's predictions and the actual data, implying a better fit. Similarly, a higher R^2 suggests that more of the variance in the model is explained by the data.

$$\text{RSS} = \sum_{i=1}^{n}(y_i - \hat{y}_i)^2 \tag{3.1}$$

$$R^2 = 1 - \frac{\sum_{i=1}^{n}(y_i - \hat{y}_i)^2}{\sum_{i=1}^{n}(y_i - \bar{y})^2} \tag{3.2}$$

y_i are the observed values, $\hat{y}_i$ are the predicted values and $\bar{y}$ the mean of the observed values.

3.3 Results

We included 66 formerly PE patients and 44 healthy controls. The baseline characteristics of the patients and controls can be found in table 1. MAP, HR, BRS, and wall-to-lumen ratio show significant differences between the two groups. We have no result of the BMI and PV/BSA of the healthy controls.

Table 1: Baseline characteristics of the total group, the formerly PE patients and the controls. The shown variables are the number of women per group (N), Body Mass Index (BMI), Age, Mean Arterial Pressure (MAP), Heart Rate (HR), plasma volume corrected for body mass (PV/BSA), Baroreceptor sensitivity (BRS), Cardiac Output (CO), Stroke Volume (SV), Vascular Resistance (VR), the difference in MAP induced by head-up tilt, the wall-to-lumen ratio of the carotid artery and the compliance of the carotid artery.

	OVERALL	FORMERLY PREECLAMPTIC	HEALTHY CONTROLS	P-VALUE
N	110	66	44	
BMI, MEDIAN [Q1,Q3]	23.1 [20.8,27.3]	23.1 [20.8,27.3]	-	-
AGE (YEARS), MEDIAN [Q1,Q3]	38.6 [36.4,40.6]	38.5 [36.6,40.0]	39.6 [36.1,42.4]	0.225
MAP (MMHG), MEDIAN [Q1,Q3]	87.2 [80.6,94.9]	90.3 [83.4,99.6]	83.7 [77.9,88.4]	<0.001
HR (BPM), MEDIAN [Q1,Q3]	63.0 [57.0,71.0]	67.0 [61.0,76.8]	60.0 [55.0,63.5]	<0.001
PV/BSA, MEDIAN [Q1,Q3]	1530.0 [1413.6,1597.2]	1530.0 [1413.6,1597.2]	-	-
BRS (MS/MMHG), MEDIAN [Q1,Q3]	13.1 [7.4,17.4]	7.9 [6.4,12.1]	17.8 [15.5,22.4]	<0.001
CO (L/MIN), MEDIAN [Q1,Q3]	6.00 [4.90,6.80]	6.10 [4.90,6.90]	5.80 [5.10,6.80]	0.795
SV (ML), MEDIAN [Q1,Q3]	93.0 [80.0,107.8]	92.0 [77.0,104.0]	97.5 [85.8,111.2]	0.077
VR (MMHG*MIN/L), MEDIAN [Q1,Q3]	16.5 [13.6,20.0]	16.9 [15.3,22.5]	15.1 [12.3,18.1]	0.004
WALL-TO-LUMEN, MEDIAN [Q1,Q3]	0.0930 [0.0807,0.1052]	0.1014 [0.0896,0.1147]	0.0811 [0.0747,0.0921]	<0.001
COMPLIANCE (MM/MMHG), MEDIAN [Q1,Q3]	0.0124 [0.0086,0.0163]	0.0105 [0.0000,0.0139]	0.0142 [0.0120,0.0176]	<0.001

We evaluated the influences of the variables for the entire group, so that possible mechanisms behind reduced BRS can be revealed. These results are shown in Figure 3. As can be seen, there is a significant correlation between MAP, HR, VR, wall-to-lumen ratio and BRS. However, the R^2 values are very small.

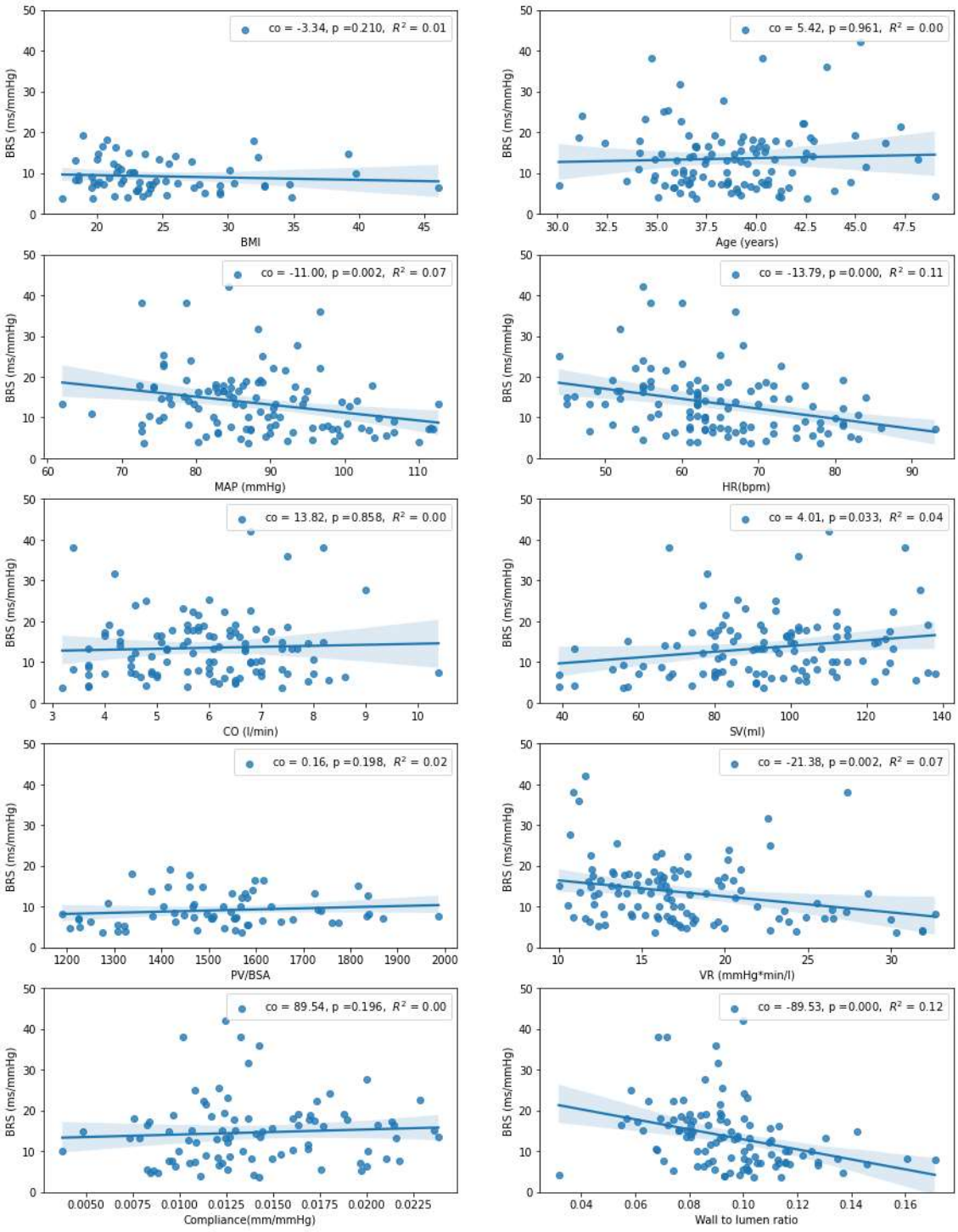

Figure 3: Relationships between body mass index (BMI), age, mean arterial pressure (MAP), heart rate (HR), cardiac output (CO), stroke volume (SV), plasma volume corrected for body surface area (PV/BSA), vascular resistance (VR), compliance, and wall-to-lumen ratio with baroreceptor sensitivity (BRS). Except for BMI and PV/BSA, the figures represent the entire group. The results of BMI and PV/BSA only show the formerly PE patients. The regression coefficients (co), p-values, and R^2 values for each variable are shown, reflecting their association with BRS across the total study population.

Next, we evaluated the formerly PE patients and healthy controls during head-up tilt measuring BRS, MAP, HR, SV, CO and VR (Figure 4). At 0 degrees tilt, PE patients exhibit significantly higher MAP (91.5 ± 11.1 mmHg) and lower BRS (9.2 ± 3.9 ms/mmHg) compared to controls (83.2 ± 7.5 mmHg; 20.0 ± 7.4 ms/mmHg) ($p<0.05$). With head-up tilt, the BP drop in PE patients is significantly more pronounced (-12.2 ± 8.5 mmHg) compared to controls (-4.4 ± 3.6 mmHg). As expected, HR rises after head-up tilt to compensate for the reduced SV and to keep sufficient CO.

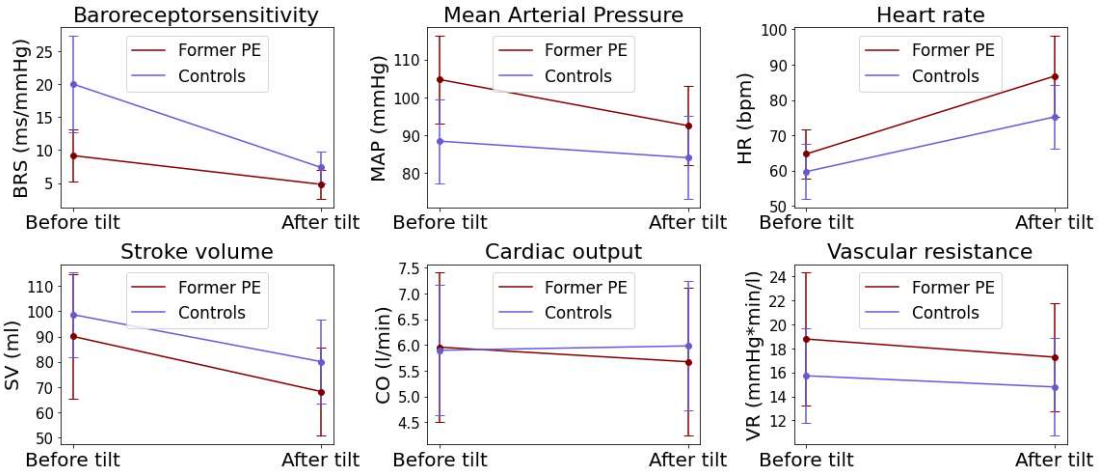

Figure 4: The baroreceptor sensitivity (BRS), Mean arterial pressure (MAP), Heart rate (HR), Stroke volume (SV), Cardiac Output (CO) and Vascular resistance (VR) measured before and after head-up tilt for formerly preeclamptic (PE) patients and healthy controls.

The decrease in MAP due to head-up tilt was significantly larger in formerly PE patients compared to healthy controls. Figure 5 shows the relationship between BRS (x-axis) and the decrease in MAP (y-axis). The figure shows that there is a notable difference in the distribution of BRS between the two groups. Formerly PE patients predominantly exhibit lower BRS values, whereas controls generally display higher BRS. The regression coefficient for the relationship between the decrease in MAP and BRS in formerly PE patients is 1.43 (ms/mmHg), which is significantly different from zero ($p < 0.05$), with an R^2 of 0.44. In contrast, the controls show a regression coefficient that is not significantly different from zero ($p = 0.154$) and an R^2 of 0.09.

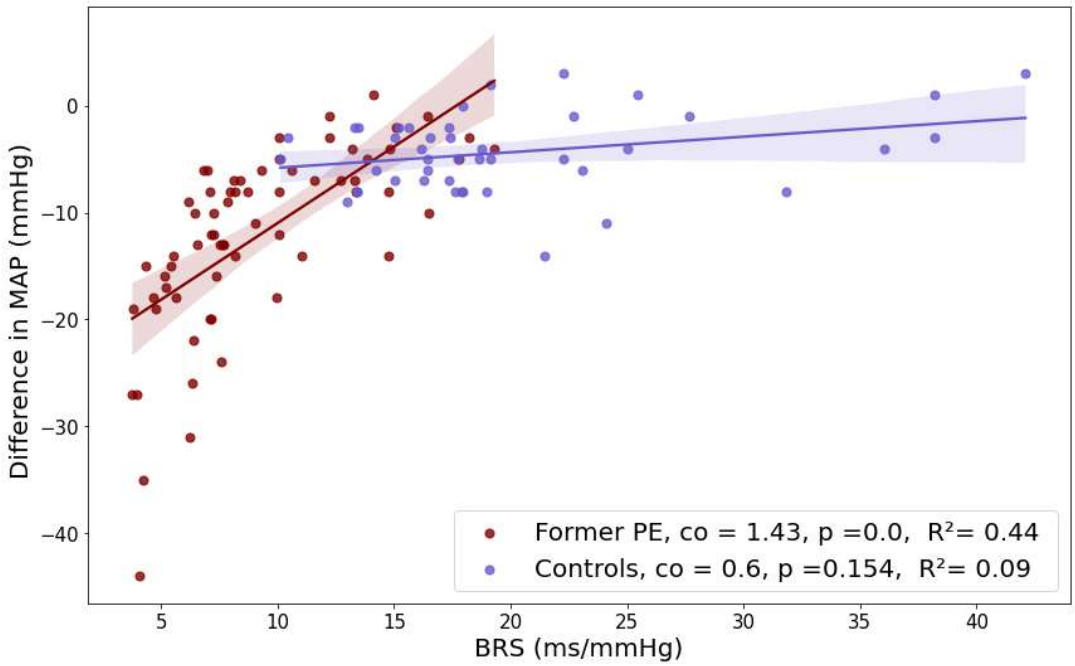

Figure 5: Linear regression of difference in mean arterial pressure (MAP) and baroreceptor sensitivity (BRS) during head-up tilt in formerly preeclamptic (PE) patients and healthy controls). The regression coefficients (co), p-values, and R^2 values for both groups are shown, reflecting their association with BRS and difference in MAP.

A logistic regression analysis has been performed on the total group to test whether a logistic regression fits the data better than linear regression, the results are shown in Figure 5. At first sight, the red line of the logistic fit seems to follow the dots better than the green line of the linear fit. The performance values shown in Table 2 confirms this.

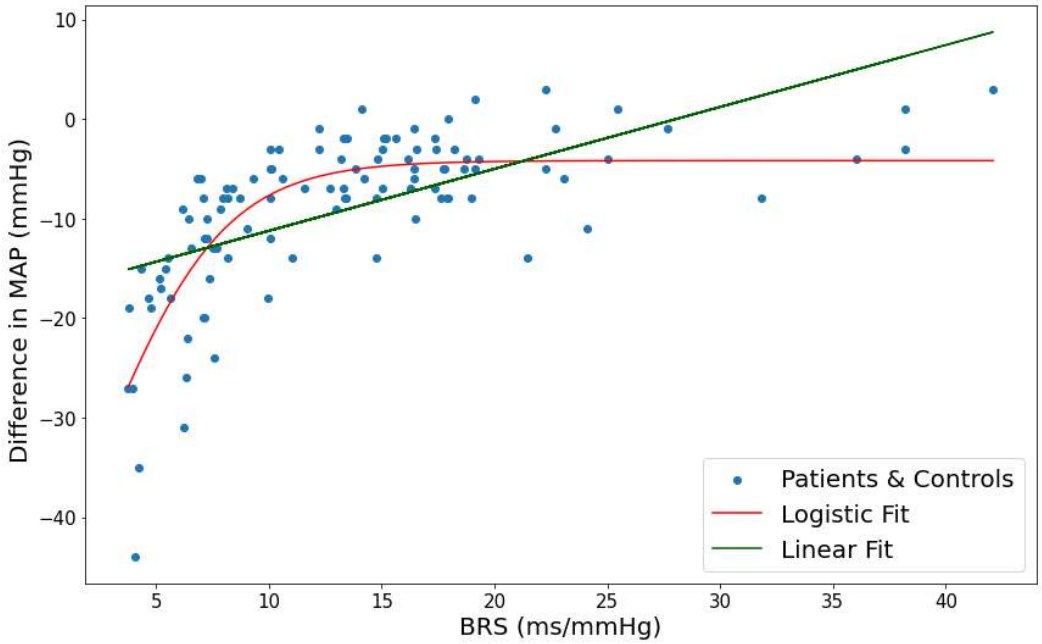

Figure 6: Logistic regression and linear regression model of decrease in mean arterial pressure (MAP) and baroreceptor sensitivity (BRS) during the tilt test fitted on the total group.

Table 2: Model performance of the correlation between baroreceptor sensitivity and the decrease in mean arterial pressure. (RSS = residual sum of squares, R^2 = the explained variance)

	Logistic model	**Linear model**
RSS	2644	4413
R^2	0.61	0.36

3.4 Discussion

In this study, we found that BRS is significantly lower in formerly PE patients compared to healthy controls, with a reduced capacity to modulate this sensitivity during head-up tilt. We investigated several cardiovascular variables to determine whether they correlated with the decreased BRS, seeking potential explanations for the impaired baroreflex function in the patient group, as well as enhancing our knowledge of the baroreflex for modeling purposes. Our analysis revealed that MAP, HR, VR, and the wall-to-lumen ratio were correlated with BRS. However, these variables accounted for only a small proportion of the variance in BRS. While it is well-established that PE can have long-term cardiovascular consequences such as a diminished BRS, our findings suggest that these cardiovascular variables may contribute to these outcomes. Nonetheless, it is evident that additional mechanisms also play a role in the reduced BRS observed in formerly PE patients.

Comparison with literature

Our findings are consistent with previous research demonstrating a reduction in BRS in individuals with a history of PE [16]. Several studies have also sought to establish correlations between BRS and various cardiovascular variables. For example, Hesse et al. reported a significant correlation between MAP and BRS with greater explained variance than ours (R^2 = 0.49; p < 0.001 vs R^2 = 0.07; p= 0.002) but they did not observe any correlation between BRS and baseline HR [17].

Despite previous evidence linking reduced plasma volume to both PE and diminished BRS [16, 18], our study did not identify a correlation between BRS and plasma volume. Moreover, while we observed a significant correlation between BRS and the wall-to-lumen ratio, we did not find a corresponding correlation between BRS and vascular compliance. This is intriguing, as will be explained later, since increased compliance is correlated to increased wall-to-lumen ratio [19], and prior studies have reported an association between compliance and BRS [20-23].

Interpretation and mechanism

The observed correlation between BRS and MAP can be interpreted through several mechanisms. Although most methods for measuring BRS primarily assess short-term regulatory responses, previous studies suggested that baroreflex activity may exert long-term influences on BP regulation. Evidence supports this notion, with data indicating that higher BRS may contribute to maintaining lower BP throughout the day. This relationship is further consistent with the understanding that reduced BRS is considered a general risk factor for cardiovascular disease, underscoring its role in long-term cardiovascular health [17]. We hypothesize that the same mechanism holds up for the correlation for BRS and HR which would explain our found correlation with BRS and HR, although this has not been reported in literature before.

The correlation between BRS and VR, as well as wall-to-lumen ratio, can be attributed to the baroreflex's activation via stretch receptors in the aortic arch. An increased wall-to-lumen ratio indicates a proportionate increase in arterial wall thickness relative to the lumen. An increase in wall thickness is associated with a reduction of the artery's compliance and thereby diminishes its capacity to stretch in response to elevations in BP [19]. This phenomenon is similar to the effects of increased VR, where more constricted arteries could exhibit reduced compliance. When VR and wall-to-lumen ratio are elevated, the reduced ability of the arterial walls to stretch in response to BP changes could lead to diminished activation of the baroreflex. However, it remains somewhat controversial that

arterial compliance itself does not appear to correlate with BRS in our study, despite previous studies proposing otherwise [20-23].

Our findings suggest that the relationship between BRS and BP modulation during the tilt test is more likely logarithmic than linear. This indicates that beyond a certain point, higher BRS does not lead to proportionally greater improvements in BP regulation. These results hint at the possibility that the baroreflex operates through more complex, non-linear mechanisms. However, a limitation of this study is that participants with lower BRS were predominantly formerly PE patients, while most controls exhibited higher BRS. As a result, it is unclear whether the observed relationships are driven by the level of BRS itself or by the presence or absence of a history of PE.

Although we did find correlations between BRS and some cardiovascular parameters, the explanatory variance of the found correlations are all considerably low. This underscores the complexity of the baroreflex and debatable results, which could explain why other studies have found different results. However, it could also be caused by different measuring and analyzing methods and different populations. Furthermore, is it likely that other mechanisms contribute to a reduction in BRS as well. One of major contributors to the baroreflex is the autonomic nervous system, specifically the sympathetic branch. Increased sympathetic activity in PE has already been reported and could play a significant role in the observed reductions in BRS [24, 25].

Strengths and limitations

A key strength of our study is the identification of potential correlations with reduced BRS. These findings contribute to the growing body of research and provide a foundation for future studies aimed at unraveling the causal mechanisms. By highlighting these associations, our study points to specific areas where research could be directed since a key limitation of this research is the inability to determine causality in the observed correlations. For instance, it is unclear whether increased MAP leads to reduced baroreflex sensitivity (BRS) or if the reverse is true. This question is especially critical in pathological conditions, where clinicians aim to treat the underlying cause rather than the symptoms. This issue is also relevant to understanding the origins of PE. Studies like ours, which focus on long-term consequences, often cannot determine whether the identified abnormalities existed prior to PE, potentially making them a cause rather than a consequence. To answer these questions, long-term follow-up studies are needed to assess whether cardiovascular risk factors are present and persist before and after PE. However, such studies are challenging and time-intensive.

3.5 Conclusion

In our study, we investigated potential mechanisms underlying the reduction in BRS observed in formerly PE patients. We found that these patients experienced a greater decrease in MAP during head-up tilt, which may be explained by the logistic relationship between BRS and the reduction in MAP. Additionally, we identified correlations between BRS and cardiovascular parameters such as MAP, HR, VR, and the wall-to-lumen ratio, though these correlations explained only a small portion of the variance. We conclude that BRS is influenced by several factors, including MAP, HR, VR, and the wall-to-lumen ratio, but its regulation is likely more complex. Other contributors, such as the autonomic nervous system, are also expected to play a significant role. Further research is needed to investigate the reduced BRS in formerly PE patients.

Chapter 4: Modeling baroreceptor mediated blood pressure control

Abstract

Objective: The baroreflex function is diminished during pregnancy, with an even greater reduction in women with hypertensive disorders. To better understand the role of the baroreflex in both healthy and hypertensive pregnancies, we aim to develop a comprehensive hemodynamic model that incorporates baroreceptor-mediated BP regulation.

Methods: We extended the lumped compartment model currently used at Radboudumc by incorporating heart rate (HR) autoregulation via the baroreflex. The parasympathetic and sympathetic branches were modeled separately, and the Bowditch effect on cardiac contractility was included. Vascular components of the baroreflex were excluded from the scope. Model validation was conducted by simulating BP alterations through arterial resistance reduction and comparing the results to head-up tilt data.

Results: The model demonstrated HR responses to BP reductions induced by decreased arterial resistance. Stroke volume decreased as HR increased, resulting in minimal changes in both cardiac output and BP. The predicted HR increase was smaller compared to the head-up tilt data.

Conclusions: We developed a closed-loop model in which heart rate (HR) responds to blood pressure (BP) alterations by independently modeling the sympathetic and parasympathetic branches of the baroreflex. Our findings indicate that isolated increases in HR, without concurrent changes in venous return or vascular tone, have a minimal effect on BP regulation. Discrepancies between our predictive data and measured data may be attributed to differences in the methods used to induce BP reduction. Further research is required to achieve comprehensive baroreflex modeling.

4.1 Introduction

Mathematical modeling is a valuable tool for studying various physiological and pathological processes. Translating complex physiological relationships and mechanisms into mathematical equations allows for precise analysis of the influence of different parameters. This approach allows researchers to address complex medical questions by simulating and testing various medical processes. In this study, we developed a model of the baroreflex, which plays a critical role in the short-term regulation of blood pressure (BP).

The baroreflex is stimulated when BP increases, triggering afferent fibers of the baroreceptors in among others the carotid sinus who signal different brain regions. The brain processes this input and generates both parasympathetic and sympathetic responses. In response to elevated BP, parasympathetic activity is enhanced, leading to the release of acetylcholine (Ach), which reduces heart rate (HR). Simultaneously, sympathetic activity is suppressed, resulting in decreased norepinephrine (NE) release, which reduces HR, cardiac contractility, and VR. Together, both branches result in a decrease in BP. The relationship between HR reduction associated with BP increase, is quantified as baroreceptor sensitivity (BRS).

Currently it is known that BRS is diminished during pregnancy, with an even greater reduction observed in pregnant women with hypertensive disorders. To better understand the role of the baroreflex in both healthy and hypertensive pregnancies, we aim to develop a comprehensive hemodynamic model that incorporates baroreceptor-mediated BP regulation.

4.2 Methods

For this study we expanded the lumped compartment model first described by Beneken et al. [26], and further advanced by researchers from the Radboudumc. However, this model does not yet include the autoregulation of HR by the baroreflex. Therefore, we performed literature research on different methods for modeling the baroreflex. which could serve as a base for our model. The most prominent requirement for modeling our baroreflex is simplicity. We required that the HR alters as a consequence of differences in BP. Furthermore, since literature shows that sympathetic influences are altered during pregnancy [5], a differentiation between the parasympathetic and sympathetic branches of the baroreflex is important, allowing us to experiment with this phenomenon. Results of the mathematical model must be repeatable and logical, where values of BP and HR lie within physiological values.

The model we chose to build upon is from Olufsen et al. [27], who in their turn based their work on the research of Ottensen et al [28] , and Seidel & Herzel [29]. For our study, we first created the model as an open-loop model, meaning that the HR determined by the baroreflex does not yet have an effect on the BP. We compared our results to that from Olufsen et al. after which we could implement our code in explain and create a close-loop model. We evaluated the function of our model by studying increase in HR and decrease in VR. We compared the closed-loop results to the data we studied in Chapter 3.

4.2.1 The lumped compartment model

The model already created by researchers from the Radboudumc will be used as the basis for this study. This is a lumped compartment model which was first described by Beneken et al. [26]. The lumped model currently used in the maternal model is shown in Figure 7. The model consists of compliances, connectors and valves. A compliance contains a volume (V) where the pressure (P) of the volume is based on the elastance (E) of the compliance and the difference between total and unstressed volume (V_0). The relationship between volume, pressure and elastance is given by equation 4.1

$$P(t) = E(t) * (V(t) - V_0)\,. \tag{4.1}$$

In the maternal model, the heart consists of four compliances, the right atrium (RA), right ventricle (RV), left atrium (LA) and left ventricle (LV) with time varying elastances. For example, during diastole, the elastance in RA and LA increase resulting in an increased pressure while the elastance in RV and LV decrease resulting in a decreased pressure. The difference in pressure, i.e. the pressure gradient, between the atria and ventricles will cause a flow from the atria to the ventricles. The equation to calculate the flow (q_{in}) is stated in Equation 4.2. The flow depends on the pressure gradient and the resistance of the connector, i.e. the connection between the two compliances. Connectors that function as valves in the heart are modeled with an infinite backwards resistance, preventing backflow from the ventricles back to the atria.

$$q_{in}(t) = \frac{1}{R} * \big(P_2(t) - P_1(t)\big). \tag{4.2}$$

When there a is flow, either in or out a compartment, the volume of the compartment changes. The equation for the change in volume is described in Equation 4.3.

$$\frac{dV(t)}{dt} = q_{in}(t) - q_{out}(t). \tag{4.3}$$

With Equations 4.1-4.3, a closed-loop system can be modeled since the output of Equation 4.3 is the input of Equation 4.1. Due to the pressure gradients created by the time varying elastances in the

heart, flow is generated from the heart towards the pulmonary and systemic circulation composing the lumped compartment model shown in Figure 7. In our maternal model, the pulmonary circulation is modeled between the RV and LA. So, the flow travels from the RV to the pulmonary arteries (PA) and the pulmonary veins (PV) back to the LA. The flow of the systemic circulation travels from the LV to the ascending aorta (AA) and the upper body and to the descending aorta (AD) and the lower body (LB). In the maternal model, the lower body is divided into circulation to and from the kidneys, uterus and the rest of the lower body. The kidneys consist of the renal arteries (AR), the glomerulus (GL), the tubule (TU) and the renal veins (VR). The uterus consists of the uterine artery (UA), spiral arteries (SA), maternal placenta (PL) and uterine veins (UV). The flow from the UB, LB, VR and UV will travel to the vena cava (VC) which brings the blood right back the heart, creating a closed-loop system.

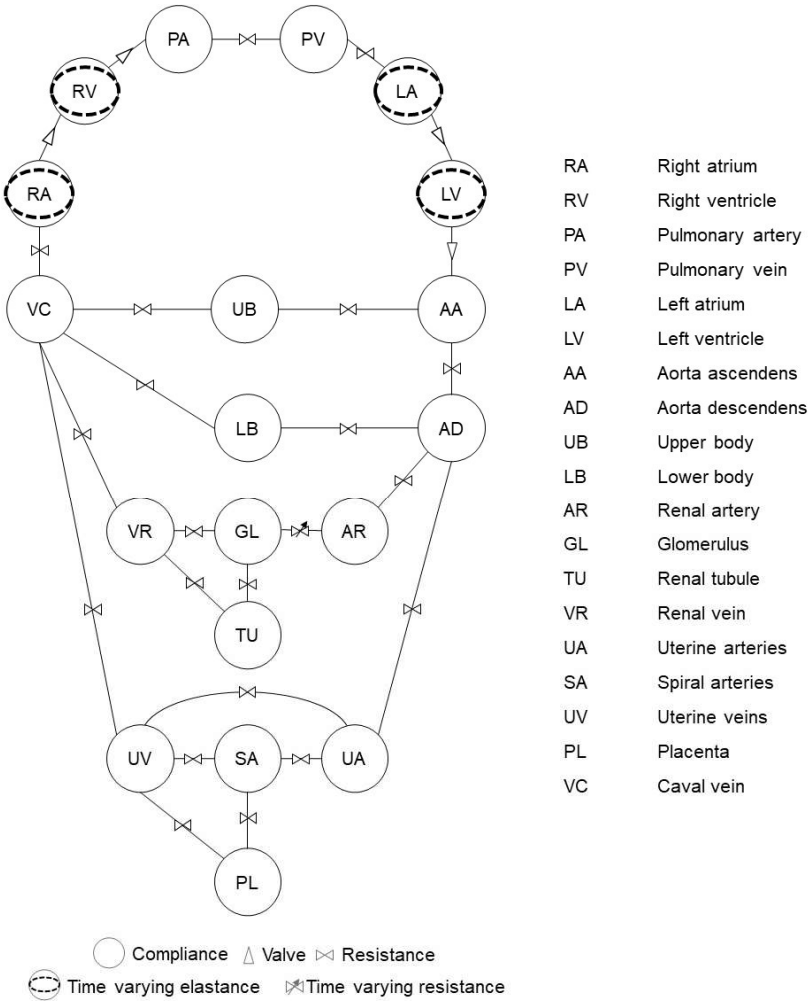

Figure 7: The lumped compartment model of the maternal cardiovascular system

4.2.2 Open-loop baroreflex model

A schematic diagram of the mathematical model used by Olufsen et al. can be seen in Figure 8 and was modelled during head-up tilt. Because, as explained earlier, head-up tilt is an ideal cardiovascular stress test for the baroreflex.

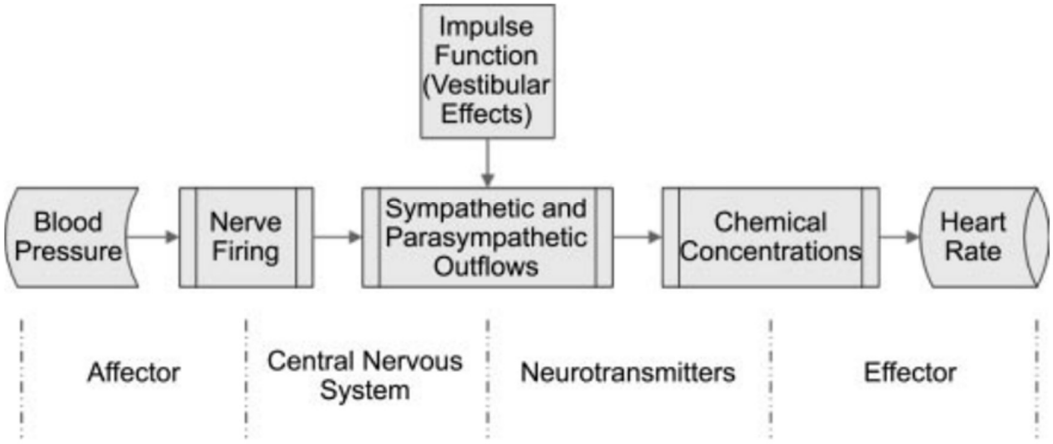

Figure 8: A schematic diagram of the baroreflex used by Olufsen et al. [27]

As Figure 8 shows, an impulse function is added to simulate the vestibular effects provoked by head-up tilt. The brain perceives changes in position via the vestibular apparatus. Next the brain signals the cardiovascular system as well as the muscular system to respond to this position change by increasing sympathetic tone. Therefore, during head-up tilt, the HR not solely increases due to a drop in BP, but also due to the position change [30]. Since it was not our goal to model head-up tilt, but rather model a resting patient, it was chosen to not include the vestibular effects into our model for the purpose of simplicity. The conceptual model we eventually used for modeling the baroreflex in open-loop is depicted in Figure 9.

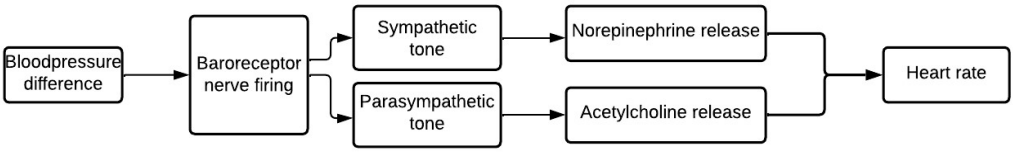

Figure 9: The conceptual model of the baroreflex.

The model starts with the *affector*, i.e. the variable which affects the output variable, the *effector.* In this case the affector is the BP and the effector the HR. We modelled that the firing rate of the baroreceptors depends on the BP differences. An increase in BP causes an increase in firing rate and vice versa. The model then increases or decreases sympathetic and parasympathetic tone based on

the firing rate. The sympathetic and parasympathetic tone will influence the neurotransmitter release (norepinephrine and acetylcholine, respectively), and the release of these neurotransmitters eventually impacts the HR.

Since the BP oscillates from beat to beat, we used the mean arterial pressure ($\bar{p}$) as input. For the open loop model, this was calculated using Equation 4.4.

$$\frac{d\bar{p}}{dt} = \alpha(p - \bar{p}). \tag{4.4}$$

a is the average parameter. Smaller values of a means more cardiac cycles used for average calculations and therefore smaller, more averaged, pressure differences. p is the actual BP measured by a sphygmomanometer in mmHg.

Afferent baroreceptor activity

Multiple baroreceptors located in the arterial wall measure the stretch caused by BP differences. The response of the baroreceptors shows several non-linearities. The firing rate increases when arterial pressure increases, but the thresholds for the different receptors vary widely. To incorporate these different thresholds in our model, three distinct characteristic time scales are used to analyze the firing rate response to BP.

This relationship between the difference in BP ($\frac{d\bar{p}}{dt}$) and firing rate (n_i) is described by Equation 4.5. The height of BP itself has not been incorporated since we only wanted to study HR differences on BP differences.

$$\frac{dn_i}{dt} = k_i \frac{d\bar{p}}{dt} \frac{n(M-n)}{(M/n)^2} - \frac{n_i}{\tau_i} \qquad with \quad 0 < n < M. \tag{4.5}$$

$i \epsilon \{S, I, L\}$ represent the different receptors, the slow S, intermediate I, and long L response. The difference in firing rate is calculated for each different baroreceptor with its own time constant (τ_i) and gain (k_i). n is the total firing rate in Hz and is described by Equation 4.6.

$$n = n_S + n_I + n_L + N. \tag{4.6}$$

If n_i = 0 firing rate n equals the baseline firing rate. M is the maximum firing rate; $\bar{p}$ (mmHg) is the mean arterial pressure calculated by differential Equation 4.4; t is time. The first term on the right-hand side, $k_i \frac{d\bar{p}}{dt} \frac{n(M-n)}{(M/n)^2}$, implies that the change in firing rate must lay within the physiological values $n = 0$ and $n = M$. The term has been introduced by the Olufsen et al. since it is non-linear, creating the effect that if n approaches M, the term will eventually decrease, with the idea that n does not extend M. However, we found that large changes in BP can still result in firing rates exceeding M or falling below 0 since no hard requirements are given. If the firing rates exceeds these physiological values, the term $\frac{n(M-n)}{(M/n)^2}$ becomes negative, which is not correct. Therefore, in our model, we limited n by including code specifying n can not be smaller than 0 or larger than M, this corresponds to the physiology. If $\frac{d\bar{p}}{dt} = 0$, the firing rate will approach 0.

The parameter values $\tau_S, \tau_I, \tau_L, k_L$ and M are based on estimates from animal studies and can be found in table 3, all other parameters were estimated using an inversed least squares problem. An inverse least squares problem calculates the differences between the computed values and the measured values.

Table 3: Parameter values obtained by Olufsen et al.

k_S [Hz/mmHg]	k_I [Hz/mmHg]	k_L [Hz/mmHg]	τ_S [s]	τ_I [s]	τ_L [s]	N [Hz]	M [Hz]	α	B [s]	λ_d [s]	τ_{nor} [s]	τ_{ach} [s]	g_{sym}	g_{par}
3.06	1.91	2.22	0.60	5.26	250	100	120	0.78	4.48	6.12	0.72	1.32	0.99	0.45

Central nervous system

Based on the firing rate, the parasympathetic (T_{par}) and sympathetic (T_{sym}) tone are calculated. The parasympathetic tone is proportional to the firing rate and is given by Equation 4.7

$$T_{par}(t) = \frac{n(t)}{M}. \tag{4.7}$$

The firing rate is divided by the maximum firing rate M so that the parasympathetic tone becomes a value between 0 and 1. The sympathetic tone is inverse to the parasympathetic tone. In case of a BP increase, parasympathetic tone rises and sympathetic tone decreases. Further it has been shown that sympathetic nervous system has a time delay of 6 to 10 seconds to show a response after a BP change while the parasympathetic tone shows a response almost immediately. Therefore, a time delay, λ_d, is incorporated in the sympathetic tone given by Equation 4.8. Sympathetic tone is inhibited by parasympathetic tone, which is dampened by a factor β

$$T_{sym}(t) = \frac{1-n(t-\lambda_d)/M}{1+\beta T_{par}(t)}. \tag{4.8}$$

Effect on heart rate

The neurotransmitters acetylcholine and norepinephrine are released by parasympathetic and sympathetic tone, respectively. In this model, the effects of the parasympathetic and sympathetic tone are limited to the release of these neurotransmitters. The release of acetylcholine (C_{ach}) is given by Equation 4.9, and the release of norepinephrine (C_{nor}) is given by Equation 4.10, τ_{ach} and τ_{nor} are time constants.

$$\frac{dC_{ach}}{dt} = \frac{-C_{ach}+T_{par}}{\tau_{ach}} \tag{4.9}$$

$$\frac{dC_{nor}}{dt} = \frac{-C_{nor}+T_{sym}}{\tau_{nor}} \tag{4.10}$$

Important to note is, as can be seen in the equations 4.9 and 4.10, parasympathetic and sympathetic tone is summed with neurotransmitter release. For this relationship to hold, the neurotransmitter release as well as the para- and sympathetic tone, must be non-dimensional, meaning it does not have a specific unit. This approach was chosen by Olufsen et al. to minimize the number of parameters that require prediction.

Eventually a decrease in BP will result in an increase in HR. This is realized by an increase in norepinephrine and sympathetic tone and a decrease in acetylcholine and parasympathetic tone. For this, an integrate-and-fire model is used where the neurotransmitters have their effect on the phase

velocity of the heart. In this context, a phase corresponds to the duration of a single heartbeat, and the phase velocity ($\frac{d\varphi}{dt}$) represents the rate at which the heart progresses through one phase. When the phase φ exceeds a value of 1, a heartbeat is triggered, and φ is reset to 0. The phase velocity is given by Equation 4.11.

$$\frac{d\varphi}{dt} = H_0\left(1 + g_{sym}C_{nor} - g_{par}C_{ach}\right). \tag{4.11}$$

H_0 = 100/60 (phases/sec) and is the intrinsic HR. This rate is due to the capability of the SA node to generate spontaneous electrical impulses without any influence from sympathetic or parasympathetic tone [11]. g_S and g_P are scaling factors for the sympathetic and parasympathetic responses. The consecutive times, t_{i-1} (s) and t_i (s), marking the times of the completion of each cardiac phase, are used to calculate the time interval between heartbeats. Dividing 60 (seconds) by this time interval yields the HR in beats per minute, which is calculated by Equation 4.12.

$$HR = 60/(t_i - t_{(i-1)}). \tag{4.12}$$

To compare our built model, we created a BP signal based on a skewed sinus to represent the BP signal of Olufsen et al. The equations can be found in Appendix A.

4.2.3 Implementation and code

The differential equations outlined in Section 4.1.1 were implemented in Python using the NumPy [31] , SciPy [32], and pandas [33] libraries. Initially, the baroreflex model was tested in an open-loop configuration within the Spyder environment. When similar results to those reported by Olufsen et al. were obtained, the code could be transcribed into a closed loop model using the Explain platform. Parameter values for elastances, capacitances, volumes, and resistances were derived from the work of van Ochten et al. [6]. Given that the objective of this research is to develop a closed-loop model, exact alignment of the open-loop results with those of Olufsen et al. was not imperative, as parameter optimization was intended to be conducted within the closed-loop framework.

To investigate the baroreflex effects, we initially examined the response of the closed-loop model to self-induced increases in HR. This approach isolated the impact of HR elevation on the model without considering additional effects that might occur if HR increases were a consequence of BP reduction. To achieve the desired outcome of increased BP following HR elevation, we incorporated the Bowditch effect into the pre-existing baroreflex model. This was necessary because without this adjustment, stroke volume (SV) would decrease excessively due to reduced filling time, eventually leading to a lower rise in cardiac output (CO) and therefore a lower rise in BP. The Bowditch effect was calculated using an activation function, where the activation factor $\alpha_{bowditch}\ (bpm)$ is calculated by Equation 4.13

$$\alpha_{\text{bowditch (t)}} = \begin{cases} sa_{HR} - op_{HR} & if\ HR(t) \geq sa_{HR} \\ HR(t) - op_{HR} & if\ th_{HR} < HR(t) < sa_{HR} \\ th_{HR} - op_{HR} & if\ HR(t) \leq th_{HR} \end{cases}. \tag{4.13}$$

The operating point (op_{HR}) is chosen 70 bmp, representing the baseline HR for the model. The saturation (sa_{HR}) was established at 120 bpm, as Bombardinie et al. have demonstrated that contractility does not further improve beyond an increase of 50 bpm above baseline [34]. They only studied increases in HR, we assumed a linear relationship and therefore chose a threshold (th_{HR}) of

40 bpm, since lower heart rates are not within the scope of this study. The contractility for each heart compartment, represented by maximal elastance, is then computed as follows:

$$E_{max,compartment} = E_{baseline,compartment} * (1 + \alpha_{\text{bowditch}} * k_{bowdicth}) \quad (4.14)$$

The baseline elastance is the elastance determined in previous research for each heart compartment [35]. The bowditch gain, $k_{bowditch}$, with a unit of bpm^{-1}, is chosen 0.01 in line with the results of Bombardini et al. So, the contractility of the heart will increase by 10% when the HR is 10 bpm above the operating point.

We applied a Savitzky-Golay filter to smooth the data since we saw noise in Figures 11 and 12, likely stemming from inherent modeling challenges. This filtering technique allowed for more accurate and objective interpretation of the results.

4.2.3 Validation

We validated our model by initiating a BP drop caused by reduced arterial resistance. We decreased the forwards and backwards resistance of the following connectors with ten percent: AA_AD, AA_UB, AD_LB, AD_AR, AD_AU. In this way, we achieved a similar drop in BP (-4 mmHg), as the head-up tilt data previously described in Chapter 3. We compared the resulting increase in HR of the head-up tilt data to our calculated HR increase. This was done by plotting the percentual change in BP and HR for both the data and our calculations, ass well ass the absolute change for BP and HR.

4.3 Results

4.3.1 Open-loop simulations

Figure 10A shows that the average BP in our model, which serves as input for the baroreflex calculations, closely aligns with the results reported by Olufsen et al., ranging from approximately 90 mmHg to 60 mmHg during head-up tilt. This consistency extends to the firing rates as well. A notable deviation occurs in Figure 10C, where parasympathetic and sympathetic tones are illustrated. Our predicted sympathetic tone lacks the initial peak observed in the model of Olufsen et al. This discrepancy arises from our decision not to incorporate the vestibulo-reflex, as previously explained. Despite this difference, we successfully replicated the findings of Olufsen et al. with near-equivalent outcomes in HR increase. Therefore, the equations and parameter values from their study are accepted for use in our closed-loop model.

4.3.2 Closed-loop simulations

Figure 11 shows how the closed loop responded on a self-initiated HR increase. We simulated a HR increase of 10 bpm. During HR increase, the graph without Bowditch effect shows that diastolic pressure increases with +2 mmHg, and systolic pressure slowly decreases with 0.5 mmHg. The graph with Bowditch effect shows an increase in systolic pressure (+1 mmHg) and diastolic pressure (+3 mmHg). SV decreases, where the reduction is more pronounced without Bowditch effect (-6 mL) compared to the simulation with Bowditch (-5 mL). CO increases more with Bowditch effect (+0.1 L/min) compared to without (+0.05 L/min), while right atrial volume decreases more with Bowditch effect (-0.85 mL) compared to without (-0.45 mL). The pressure in the vena cava increases with 0.05 mmHg and is more or less the same for both circumstances.

Next, we assessed the model's response to a BP reduction induced by a self-imposed decrease in arterial resistance (Figure 12). Results were compared across three scenarios: with the baroreflex activated, with the baroreflex deactivated, and with the baroreflex activated but excluding the Bowditch effect. The systolic BP exhibited a comparable decline across all three conditions. The drop in diastolic pressure was less pronounced (-2 mmHg) in the activated baroreflex models compared to the deactivated model (-2.5 mmHg), although the pressure eventually attenuated toward lower pressure levels over time. HR increased in both baroreflex-activated scenarios with 1.5 bpm. In the activated baroreflex models, SV initially decreased but subsequently rose above baseline levels while in the de-activated model, SV increased directly. CO increased across all three scenarios, the baroreflex model incorporating the Bowditch effect produced the greatest increase although differences were marginal. The volume in the right atrium increased in all three models, with the deactivated baroreflex scenario exhibiting the largest increase. The pressure in the vena cava rises the same for the activated model, the de-activated model shows a less pronounced increase.

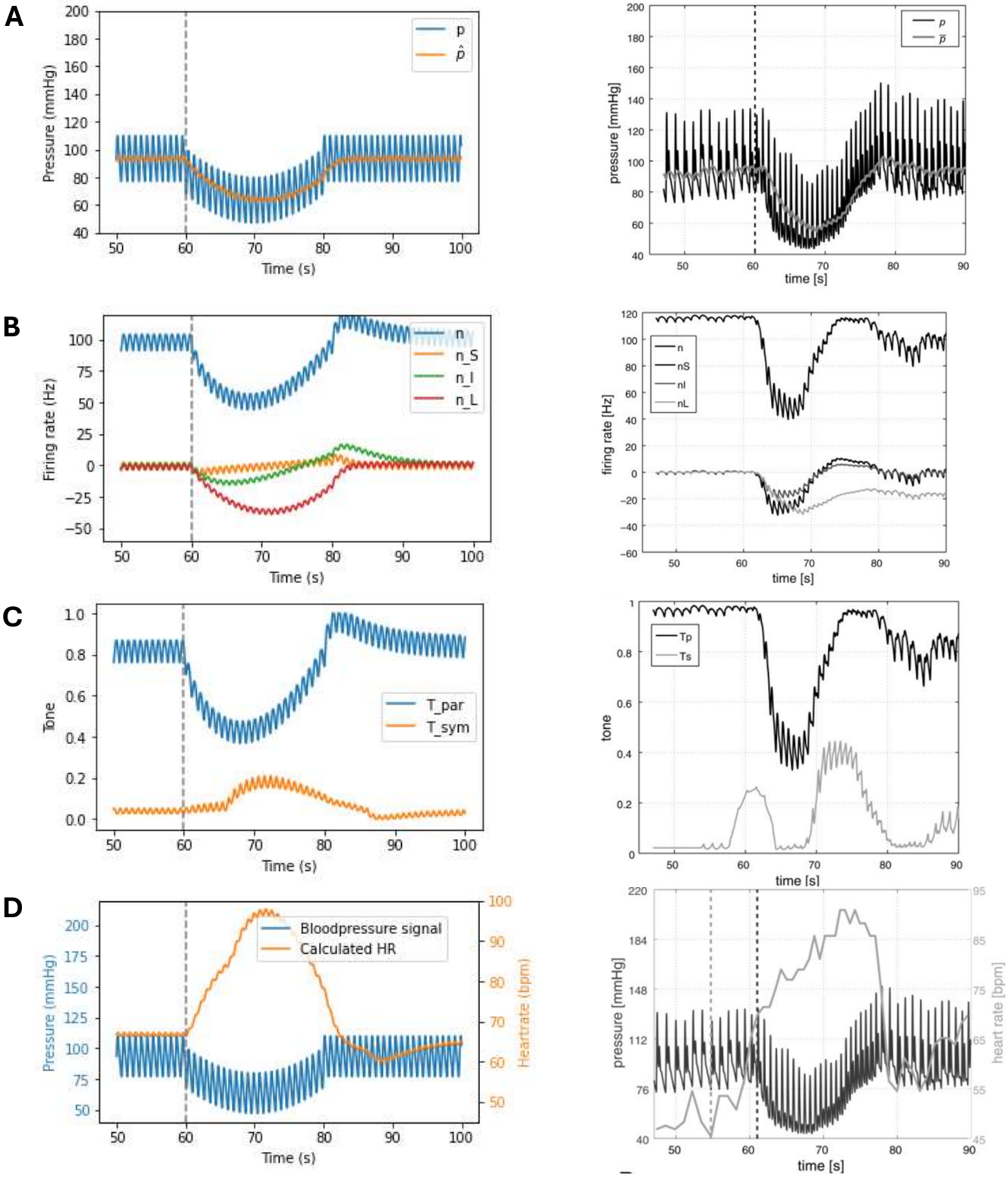

Figure 10: The comparison of our results(left) to those of Olusen et al. (right). On t =60, the BP drop is initiated, marked with a grey dashed line. A: the blood pressure p over time, toghether with the averaged blood pressure $\hat{p}$. B: the total firing rate n, and the slow (n_S), intermidiate(n_I) and long (n_L) firing rates. C: the parasympathic and sympathetic tone. D: the blood pressure on the left axis and heart rate on right axis.

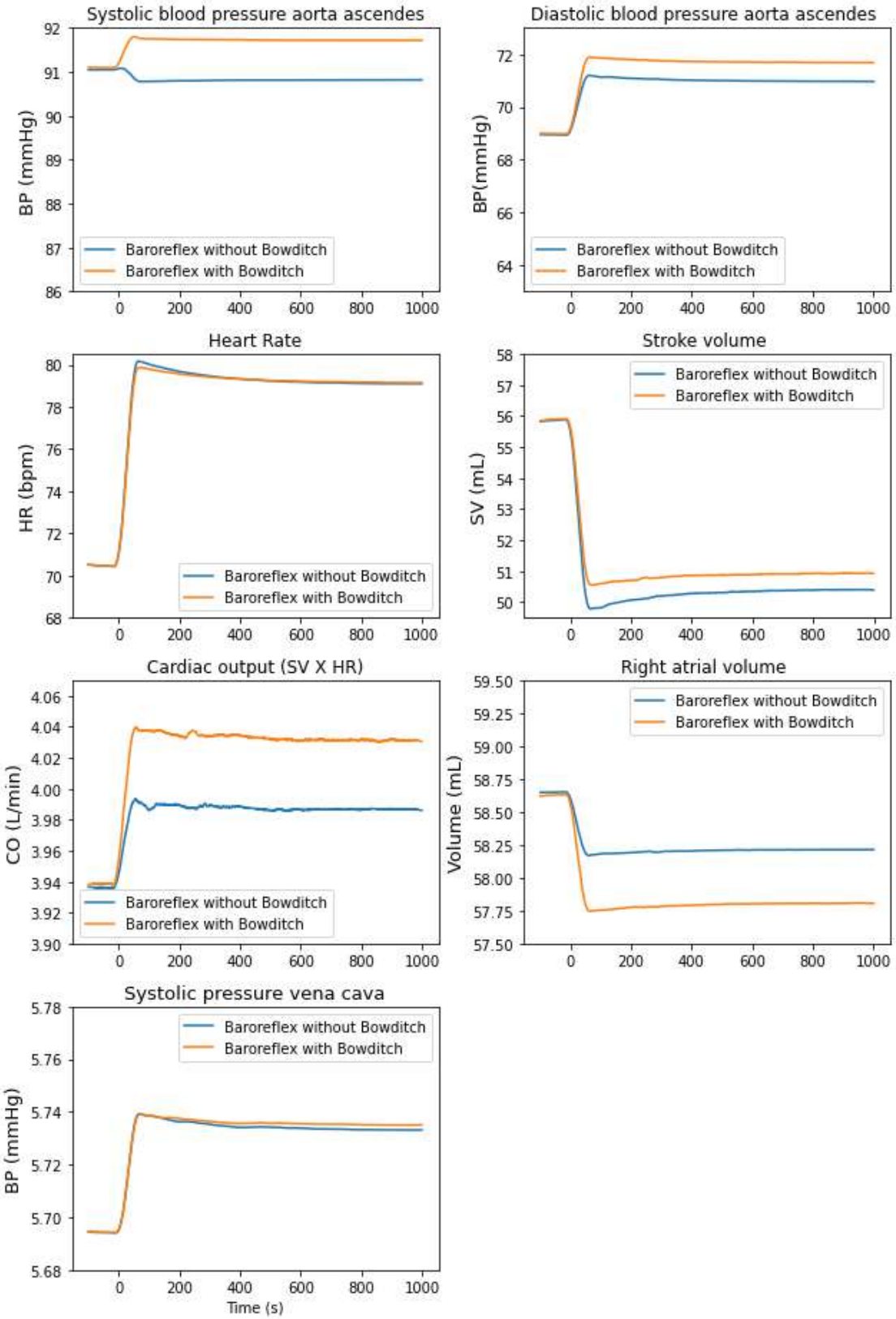

Figure 11: The systolic and diastolic blood pressure in the aorta ascendens, heart rate, stroke volume, cardiac output, right atrial volume and systolic pressure in the vena cava plotted during a self-initiated heart rate increase at t=0 without (blue) and with (orange) Bowditch.

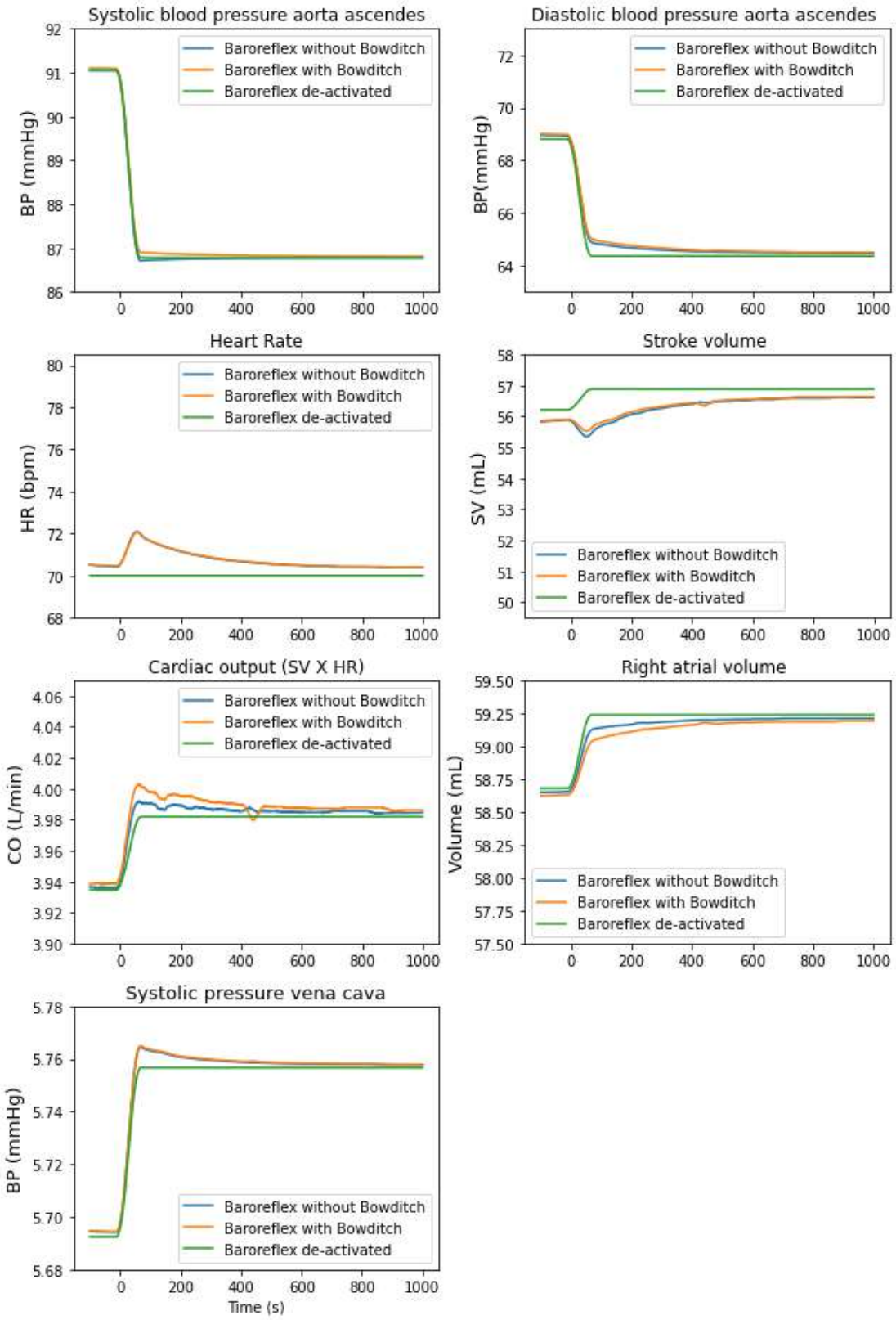

Figure 12: The systolic and diastolic blood pressure in the aorta ascendens, heart rate, stroke volume, cardiac output and right atrial volume plotted during a decrease in arterial vascular resistance at t=0.

For validation, we compared BP and HR data from the head-up tilt to the BP drop induced by alterations in vascular resistance (VR) in our model. As illustrated in Figure 13A, while the decrease in MAP is consistent across both, the HR increase observed in the head-up tilt data is approximately 20% higher than in our model's predictions. Figure 13B displays the absolute change in HR, where the head-up tilt data begins at a lower baseline (60 bpm) and exhibits a larger increase (+15 bpm) compared to the predicted HR (70 + 3 bpm). Similarly, Figure 13C illustrates the absolute change in mean arterial pressure (MAP), showing that while the overall decline is the same, our predicted MAP starts 12 mmHg lower that the head-up tilt data. This is because the MAP in our model is calibrated on a specific value by various parameters and cannot easily be adjusted.

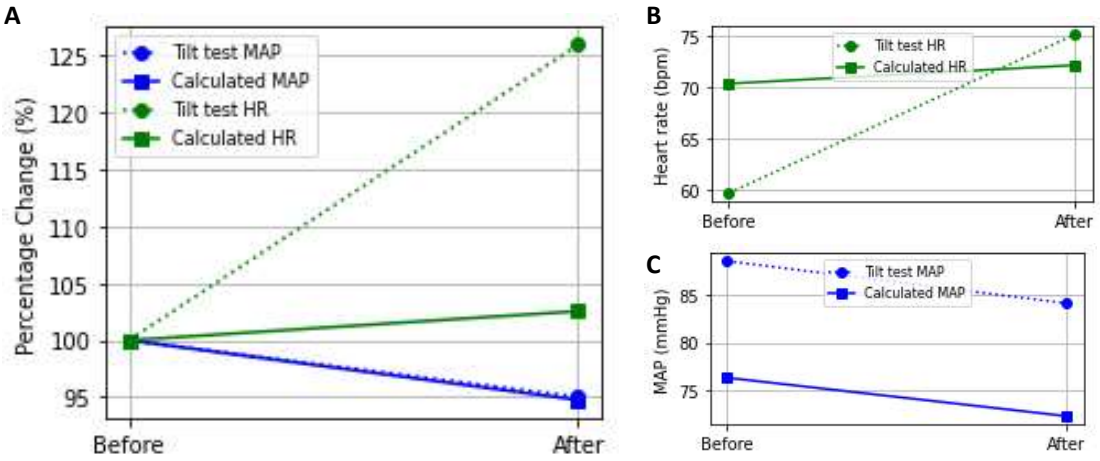

Figure 13A: Percental change before and after blood pressure intervention for the head-up tilt data and our calculated data. B: Heart rate values before and after blood pressure intervention. C: Mean arterial pressure values before and after blood pressure intervention.

4.4 Discussion

In this study, we developed a closed-loop model for BP regulation with a novel integration of both sympathetic and parasympathetic tone in the baroreflex response, focusing on insights relevant to pregnancy. The model was based on a lumped compartment framework, utilizing well-established relationships between pressure, elastance, and flow. A novel aspect of our approach involved incorporating the baroreflex focused on the regulation of HR as a function of BP. Specifically, the model captures the physiological response of increased HR and contractility based on sympathetic and parasympathetic tone in response to a drop in BP, a response analogous to those observed during pregnancy. The VR adaptation of the baroreflex has not been incorporated into our model due to time challenges. Our findings indicated that increases in HR, without concurrent changes in venous and arterial tone, exert minimal influence on BP regulation.

Comparison to literature

Various mathematical models integrating closed-loop baroreflex control have been proposed, each addressing different complexities of the cardiovascular system by emphasizing and simplifying particular aspects. We aimed at eventually creating a comprehensive maternal hemodynamic model, therefore we emphasized on possible cardiovascular challenges of pregnancy in our model, such as the sympathetic and parasympathetic tone of the baroreflex. The mathematical framework of the baroreflex we employed builds upon previous research by Olufsen et al., which we incorporated into a closed-loop system.

Other studies modeling the baroreflex have focused primarily on cellular or neural processes. These studies examined ionic currents involved in the baroreflex, simulating the initiation and propagation of action potentials [8]. Others concentrated on the interactions between various brain regions associated with the baroreflex and their integration with respiratory functions [36]. Additionally, some research explored calcium transport and molecular mechanisms [7], or specifically investigated either the sympathetic [37], or parasympathetic pathways [9].For our study, the autonomic nervous system is of particular interest, given the proposed alterations during pregnancy. However, the highly detailed cellular and molecular mechanisms examined in these studies are less relevant to our focus. Our maternal model aims to simulate the modulation and distribution of blood volume and BP at a macroscopic level, which aligns more closely with the broader physiological changes occurring during pregnancy.

The studies by Sharifi et al. and Jezek et al. bear the most similarity to our work, as they both tested BP across multiple compartments and under various conditions. Sharifi et al. emphasized the importance of vascular tone in baroreflex modeling, reporting results comparable to ours in their prototype model, which, like ours, did not incorporate the vascular component of the baroreflex on firsthand [7]. Furthermore, Jezek et al. demonstrated that the absence of baroreflex activation leads to a more pronounced decrease in arterial pressure, corresponding to our results [9]. Both studies provide valuable examples that could inform the further development of our baroreflex model. What sets our study apart from these previous works is the incorporation of both branches of the autonomic nervous system, a feature missing from the aforementioned models. By integrating both the sympathetic and parasympathetic pathways, our model offers a more comprehensive framework for studying baroreflex regulation under various physiological and pathophysiological conditions, including pregnancy.

Interpretation and mechanism

An increase in HR typically elevates CO by increasing the frequency by which blood is pumped into the vascular system. However, for this to be effective, the heart must have sufficient time to fill between beats. As HR increases, the filling time decreases, potentially leading to a reduction in SV if venous return does not increase as well. Sharafi et al. have also encountered this phenomenon when they only modeled the chronotropic effects of the baroreflex [7]. In our model, when we increased HR, we observed only a slight rise in diastolic pressure, while systolic pressure actually decreased, which is shown in Figure 11. This outcome can be explained by the reduced SV as explained above. We showed a decreased right atrial volume, which is caused by the reduced filling time, resulting in reduced SV. Although CO increased due to the higher HR, the increase was marginal. The discrepancy between the slight diastolic rise and systolic fall of pressure can also be explained by the reduced SV but increased CO. During systole, less blood is pumped into the system, decreasing systolic pressure. The diastolic pressure does increase because the increased CO over time will eventually result in increased blood volume within the vascular system. When the Bowditch effect was incorporated into the model, we observed an increase in diastolic as well as systolic BP. This is due to the slight increase in SV associated with the enhanced contractility that characterizes the Bowditch effect.

We tested our baroreflex model by simulating a drop in BP initiated by a reduction in VR. The results showed decreases in both systolic and diastolic pressures, although the drop in diastolic pressure was less pronounced, shown in Figure 12. In response to the decreased BP, the HR increased, as expected, with a corresponding decrease in SV, together leading to a slight increase in CO.

We evaluated the model by comparing results with and without baroreflex activation, as well as with and without the Bowditch effect. The most promising results were observed when the baroreflex with Bowditch effect was activated, which led to the smallest decrease in arterial BP, shown in Figure 12. Interestingly, when BP decreased without baroreflex activation, SV increased. However, since HR remained constant, the overall increase in CO was smaller compared to when the baroreflex was active. This increase in SV can be attributed to an accumulation of blood in the venous compartment seen as increased pressure in the vena cava. The increased volume and pressure in the vena cava cause increased venous return, which results in increased right atrial volume.

In the model, diastolic pressure under baroreflex control gradually converged with the diastolic pressure observed without baroreflex activation. This behavior can be explained by the transient nature of the HR increase in response to BP reduction. In our model, HR is regulated solely by differences in BP rather than by the absolute level of BP, as our focus was on short-term BP regulation. Consequently, as BP approaches its lowest point following a reduction in VR, HR returns to the baseline HR. If HR had remained elevated, BP would have been sustained at higher levels.

We sought to validate our model using head-up tilt data; however, our predicted values did not correspond to the measured data. Specifically, we observed a 20% greater increase in HR in the experimental data compared to our model's predictions for the same decrease in BP. While our model produced HR responses similar to those reported by Olufsen et al., whose equations and parameter values we adopted, several factors likely contribute to the observed discrepancies of our simulated and measured data. First, the input conditions of the models differ slightly, and the physiological mechanisms underlying a head-up tilt test are inherently distinct from those associated with a reduction in VR. In the head-up tilt data, measurements were taken five minutes post-tilt, a time frame that allows for partial stabilization of BP and HR. In contrast, our model is designed to simulate immediate effects and short-term regulatory responses. Second, the initial conditions and parameter values of our model were derived from the data used by Olufsen et al., where we indeed observed

comparable results. For optimal validation of our model, real-time data on HR and BP during rest would be more appropriate. Without such data, incorporating the fluid redistribution that accompanies the tilt test into our model would be necessary, which falls beyond the intended scope of our current work.

Strengths and limitations

A notable strength of this study lies in its comprehensive incorporation of both the sympathetic and parasympathetic branches of the baroreflex. In addition, our model is based on previous research making it more reliable. The model we developed dynamically adjusts heart rate (HR) in response to fluctuations in blood pressure (BP), enhancing its applicability in simulating physiological responses.

However, the study also has several limitations. As previously noted, the vascular branch of the baroreflex is not included in our model, and HR adjustments are made solely in response to BP changes without consideration of baseline HR. Furthermore, Equation 4.5 may be unnecessarily complex, despite yielding results within physiological parameters. This complexity arises because the firing rate differential is influenced by the firing rate itself through a complex term involving the maximum firing rate. Simplifying this equation—potentially by employing an activation function akin to that in Equation 4.13—could make the model more intuitive and accessible.

Future recommendations

The next step in advancing our model is the incorporation of baroreflex-mediated adaptations, specifically the regulation of arterial and venous resistance, as well as cardiac contractility, so that physiology is closely mimicked. In this way we enable more reliable simulations and create opportunities for testing other physiological or pathological phenomena. Further we should perform parameter optimization using real-time BP and HR data whereafter validation could be followed. Furthermore, it should be considered to not only let the HR depend on differences in BP, but also absolute values of BP. Moreover, the investigation of BRS should not be limited to its attenuation alone, as BRS could be considered a dynamic parameter rather than a fixed setpoint, as we observed large variability of BRS during head-up tilt. The variability of BRS may play a critical role in both physiological and pathological processes, highlighting its potential significance beyond static regulation [38].

Following the integration of these mechanisms, the model can be applied to investigate hemodynamic changes during pregnancy. For accurate pregnancy simulations, it is essential to account for HR adaptation based on circulating blood volume, rather than relying solely on BP. This is because during pregnancy, BP drops but blood volume increases. This increase in blood volume should increase HR to ensure adequate blood circulation and maintain cardiovascular stability. Promising areas for further exploration include the impact of increased sympathetic activity and the attenuation of BRS, both seen in healthy and complicated pregnancy.

Once the remaining branches of the baroreflex have been integrated into the mathematical model, it will provide an ideal platform to test the correlations identified in Chapter 3 and assess whether these relationships hold or shift under more comprehensive simulations. This will offer valuable insights into the underlying mechanisms of the baroreflex.

Clinical relevance

The primary objective of this research is to enhance an existing hemodynamic model by incorporating baroreflex mechanisms to eventually enable evaluation of maternal hemodynamic changes. This evaluation is particularly crucial, as BP-related complications during pregnancy, such as PE, are associated with high morbidity and pose significant risks to maternal and fetal health. Through this work, we have moved closer to integrating the baroreflex into the model, an essential step in

understanding and simulating the maternal cardiovascular changes. In clinical practice, an enhanced understanding of maternal hemodynamics could lead to more personalized management of BP complications such as PE. By simulating different physiological scenarios, our model could also assist in predicting adverse outcomes and training healthcare professionals in managing high-risk pregnancies.

4.5 Conclusion

This study developed a closed-loop model of BP regulation, incorporating both sympathetic and parasympathetic branches of the autonomic nervous system, offering a more comprehensive framework for simulating cardiovascular dynamics, especially in the context of pregnancy. Our findings demonstrate that isolated increases in HR without concurrent adjustments in venous return or vascular tone have minimal impact on BP regulation, a result that underscores the importance of a fully integrated baroreflex response. While the model successfully simulates short-term cardiovascular responses, further development is needed to incorporate venous and arterial adaptations for more accurate simulation of maternal hemodynamic changes during pregnancy. Future work will focus on refining the model to include baroreflex-mediated vascular adaptations and parameter optimization using real-time clinical data, bringing us closer to a tool that can predict and simulate BP-related complications in pregnancy, such as preeclampsia, to ultimately improve maternal and fetal health outcomes.

Bibliography

1. Sanghavi, M. and J.D. Rutherford, Cardiovascular Physiology of Pregnancy. Circulation, 2014. 130(12): p. 1003-1008.
2. Dimitriadis, E., et al., Pre-eclampsia. Nat Rev Dis Primers, 2023. 9(1): p. 8.
3. Andreas Voss a, H.M.a.A.S.a.N.W.a.T.W.b.H.S.c.R.F.c., Baroreflex sensitivity, heart rate, and blood pressure variability in normal pregnancy. 2000.
4. Helayne M. Silver, M., Kari U.O. Tahvanainen, MSc, Tom A. Kuusela, PhD, and and M. Dwain L. Eckberg, Comparison of vagal baroreflex function in nonpregnant women and in women with normal pregnancy, preeclampsia, or gestational hypertension. 2000.
5. Brooks, V.L., et al., Chapter 3 - Adaptations in autonomic nervous system regulation in normal and hypertensive pregnancy, in Handbook of Clinical Neurology, E.A.P. Steegers, M.J. Cipolla, and E.C. Miller, Editors. 2020, Elsevier. p. 57-84.
6. van Ochten, M., et al., Modeling renal autoregulation in a hemodynamic, first-trimester gestational model. Physiological Reports, 2022. 10(19): p. e15484.
7. Sharifi, H., et al., A multiscale model of the cardiovascular system that regulates arterial pressure via closed loop baroreflex control of chronotropism, cell-level contractility, and vascular tone. Biomechanics and Modeling in Mechanobiology, 2022. 21(6): p. 1903-1917.
8. Fernandes, L.G., et al., Closed-loop baroreflex model with biophysically detailed afferent pathway. International Journal for Numerical Methods in Biomedical Engineering, 2024. n/a(n/a): p. e3849.
9. Jezek, F., et al., Systems analysis of the mechanisms governing the cardiovascular response to changes in posture and in peripheral demand during exercise. Journal of Molecular and Cellular Cardiology, 2022. 163: p. 33-55.
10. Swenne, C.A., Baroreflex sensitivity: mechanisms and measurement. 2013.
11. Boron and Boulpaep, Medical Physiology A cellular and molecular approach. 2012: Elsevier.
12. Electrophysiology, T.F.o.t.E.S.o.C.t.N.A.S.o.P., Heart Rate Variability. Circulation, 1996. 93(5): p. 1043-1065.
13. Hayano, J. and E. Yuda, Pitfalls of assessment of autonomic function by heart rate variability. J Physiol Anthropol, 2019. 38(1): p. 3.
14. Lanfranchi, P.A. and V.K. Somers, Chapter 20 - Cardiovascular Physiology: Autonomic Control in Health and in Sleep Disorders, in Principles and Practice of Sleep Medicine (Fifth Edition), M.H. Kryger, T. Roth, and W.C. Dement, Editors. 2011, W.B. Saunders: Philadelphia. p. 226-236.
15. de Haas, S., et al., Blood pressure adjustments throughout healthy and hypertensive pregnancy: A systematic review and meta-analysis. Pregnancy Hypertens, 2022. 27: p. 51-58.
16. Courtar, D.A., et al., Low plasma volume coincides with sympathetic hyperactivity and reduced baroreflex sensitivity in formerly preeclamptic patients. J Soc Gynecol Investig, 2006. 13(1): p. 48-52.
17. Hesse, C., et al., Baroreflex sensitivity inversely correlates with ambulatory blood pressure in healthy normotensive humans. Hypertension, 2007. 50(1): p. 41-6.
18. Heidema, W.M., et al., Venous and autonomic function in formerly pre-eclamptic women and controls matched for body mass index. Ultrasound Obstet Gynecol, 2019. 53(3): p. 376-382.
19. Nakamura, M., et al., Reduced vascular compliance is associated with impaired endothelium-dependent dilatation in the brachial artery of patients with congestive heart failure. J Card Fail, 2004. 10(1): p. 36-42.
20. Colaci, M., et al., Reduction of carotid baroreceptor sensitivity in systemic sclerosis. Clinical and Experimental Rheumatology, 2022. 40(10): p. 1964-1969.
21. Desai, V.S., et al. Interaction of large artery stiffness and baroreceptor function explored through multiple measurement techniques-a pilot study. in Proceedings of the Annual

International Conference of the IEEE Engineering in Medicine and Biology Society, EMBS. 2023.
22. Eveson, D.J., et al., Abnormalities in cardiac baroreceptor sensitivity in acute ischaemic stroke patients are related to aortic stiffness. Clinical Science, 2005. 108(5): p. 441-447.
23. Tomoto, T., et al., Midlife aerobic exercise and dynamic cerebral autoregulation: associations with baroreflex sensitivity and central arterial stiffness. J Appl Physiol (1985), 2021. 131(5): p. 1599-1612.
24. Moors, S., et al., Heart rate variability in hypertensive pregnancy disorders: A systematic review. Pregnancy Hypertens, 2020. 20: p. 56-68.
25. Yousif, D., et al., Autonomic Dysfunction in Preeclampsia: A Systematic Review. Front Neurol, 2019. 10: p. 816.
26. Beneken, J.E.W., A mathematical approach to cardio-vascular function. Rijksuniversiteit Utrecht, 1965.
27. Olufsen, M.S., et al., Modeling baroreflex regulation of heart rate during orthostatic stress. Am J Physiol Regul Integr Comp Physiol, 2006. 291(5): p. R1355-68.
28. Ottesen, J.T., Modelling the dynamical baroreflex-feedback control. Mathematical and Computer Modelling, 2000. 31(4): p. 167-173.
29. Seidel, H. and H. Herzel, Modelling Heart Rate Variability Due to Respiration and Baroreflex. 1994.
30. Di Rienzo, M., et al., Baroreflex contribution to blood pressure and heart rate oscillations: time scales, time-variant characteristics and nonlinearities. Philosophical Transactions of the Royal Society A: Mathematical, Physical and Engineering Sciences, 2009. 367(1892): p. 1301-1318.
31. Harris, C.R., et al., Array programming with NumPy. Nature, 2020. 585(7825): p. 357-362.
32. Virtanen, P., et al., SciPy 1.0: fundamental algorithms for scientific computing in Python. Nature Methods, 2020. 17(3): p. 261-272.
33. McKinney, W., Data Structures for Statistical Computing in Python. 2010. 56-61.
34. Bombardini, T., Myocardial contractility in the echo lab: molecular, cellular and pathophysiological basis. Cardiovascular Ultrasound, 2005. 3(1): p. 27.
35. van Ochten, M., Modeling renal autoregulation in a hemodynamic, mathematical model of a pregnant woman.
36. Gee, M.M., et al., Closed-loop modeling of central and intrinsic cardiac nervous system circuits underlying cardiovascular control. AIChE Journal, 2023. 69(4): p. e18033.
37. Yao, Y. and M.V. Kothare, Nonlinear Closed-Loop Predictive Control of Heart Rate and Blood Pressure Using Vagus Nerve Stimulation: An In Silico Study. IEEE Transactions on Biomedical Engineering, 2023. 70(10): p. 2764-2775.
38. Zamir, M., et al., Baroreflex variability and “resetting”: A new perspective. Journal of Biomechanics, 2014. 47(1): p. 237-244.

Appendix A

The oscillatory signal $y(t)$, representing systole and diastole, is defined by Equation A.1. A skew factor was introduced to account for the fact that the rise in BP during systole occurs more rapidly than its decline during diastole, as illustrated in Figure A1. To achieve physiological BP values, the signal $y(t)$ is first shifted by adding one, ensuring all values are positive. Next, it is scaled by $\frac{(P_{sys}-P_{dias})}{2}$ to set the appropriate amplitude of the oscillations, and the diastolic pressure is added to establish the signal's baseline, this is calculated in Equation A.2. Finally, a parabolic component, given by Equation A.3, is incorporated to simulate the BP drop.

$$y(t) = \left(sin(2\pi ft + K_{skew} * sin(2\pi ft))\right) \tag{A.1}$$

$$P(t) = (y+1) * \frac{(P_{sys}-P_{dias})}{2} + P_{dias} + Parabola \tag{A.2}$$

$$Parabola = \begin{cases} a * (t - t_{start}) * (t - t_{end}) + b & if IntervalStart < t < IntervalEnd \\ 0 & Otherwise \end{cases} \tag{A.3}$$

The frequency f (Hz) is the baseline HR frequency calculated by $f = \frac{HR}{60}$ to represent systole and diastole. The baseline HR for our model was chosen as 70 bpm. The k_{skew} was set to 0.5. P_{sys} was chosen 110 mmHg, and P_{dias} 77 mmHg, corresponding to the values of Olufsen et al. To simulate a BP drop of ~ 35 mmHg, the parameter values a and b for the parabola were set 0.21 and 30, respectively. Note that a has units of mmHg*sec^{-2}.

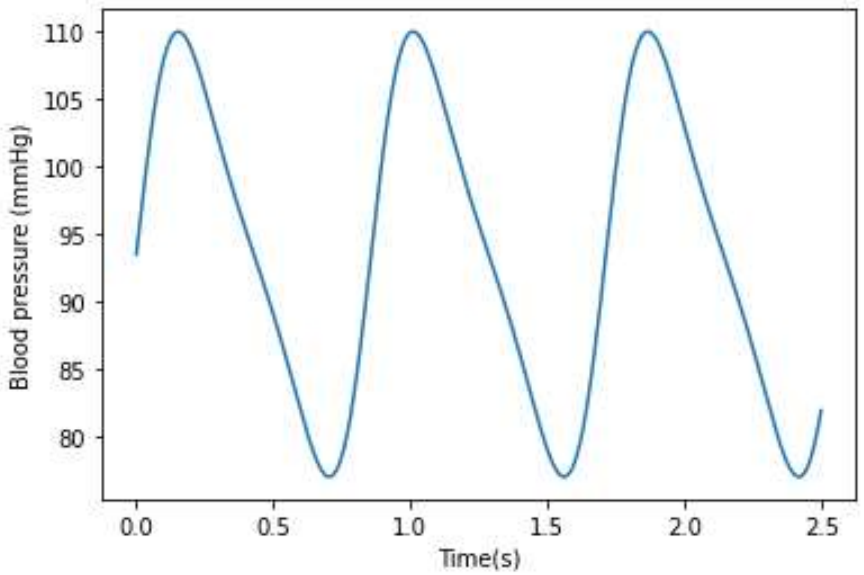

Figure A1: The skewed sinus used for creating a blood pressure signal.